CENTRO DE INVESTIGACION Y DE ESTUDIOS AVANZADOS DEL INSTITUTO POLITECNICO NACIONAL

Unidad de Genómica Avanzada

"Genetic characterization of *Med12* genes in maize"

Thesis submitted by:
Biol. Ana Laura Alonso Nieves

To obtain the degree of:
Master in Science

Specializing in:
Plant Biotechnology

Supervised by:

C. Stewart Gillmor III, Ph.D. **Ruairidh J. Hay Sawers, Ph.D.**

Irapuato, Guanajuato August, 2017

CENTRO DE INVESTIGACION Y DE ESTUDIOS AVANZADOS DEL
INSTITUTO POLITECNICO NACIONAL

Unidad de Genómica Avanzada

"Caracterización de los genes *Med12* en maíz"

Tesis que presenta:
Biol. Ana Laura Alonso Nieves

Para obtener el grado de:
Maestría en Ciencias

En la especialidad de:
Biotecnología de Plantas

Codirectores de Tesis:

Dr. C. Stewart Gillmor III **Dr. Ruairidh J. Hay Sawers**

Irapuato, Guanajuato Agosto, 2017

Agradecimientos

Al Consejo Nacional de Ciencia y Tecnología (CONACyT) por el financiamiento otorgado para la realización de este proyecto de investigación.

Al Centro de Investigación y Estudios Avanzados del IPN, Unidad Irapuato por facilitar los recursos necesarios para llevar acabo esta investigación.

A Stewart Gillmor y Ruairidh Sawers por darme la oportunidad de trabajar en su laboratorio, por la confianza y por todo lo que me han enseñado.

A los miembros del comité: Dr. Luis Herrera y Dr. Axel Tiessen, por sus valiosos y oportunos comentarios que enriquecieron este trabajo.

A los actuales y ex-miembros de los laboratorios de Desarrollo y Morfogenesis de Plantas, y de Genética y Genómica del maíz (por orden alfabético): Alma, Beatriz, Carol, Carolina, Chío, Christian, Daniel, Dario, Edith, Eliécer, Elsa, Elvira, Erick, Gerardo, Jaime, Jessy, Juan, Karla, Manuel, Marcelina, Michael, Nancy, Sofia, Vladimir.

A todos mis amigos del cinvestav.

Contents

List of Figures

List of Tables

Resumen

Mediador es un complejo multiproteínico altamente conservado en todos los eucariontes, que funciona como un activador o represor transcripcional. Regula diferentes procesos fisiológicos y del desarrollo, tales como el tiempo de desarrollo, organogénesis, respuesta a hormonas y la respuesta a estres biótico y abiótico. Esta organizado en diferentes módulos: la cabeza, el medio y la cola; así como el módulo desmontable llamado CDK8, el cual consiste en MED12, MED13, CDK8 y CYC C. En trabajos anteriores mostraron que algunos miRNAs que responden a carencia de fósforo, como miR827, miR397, miR398, se encuantran sobre expresados en las mutantes *med12* de Arabidopsis cuando crecen en condiciones optimas de fósforo. Además, aproximadamente 40 miRNAs involucrados en la arquitectura del sistema radicular y en mofogénesis, y 11 miRNAs que responden a estrés ambiental mostraron cambios de expresión, sugiriendo que *Med12* tiene un papel importante en el desarrollo de la raíz y en general, en la respuesta al ambiente. El maíz tiene dos genes paralogos *Med12*, los cuales fueron llamados *ZmMed12a* y *ZmMed12b*, ambos se expresan en toda la planta. Para conocer las funciones de estos genes, se generaron mutantes insersionales utilizando dos sistemas de transposones, *Ac/Ds* y *Mutator*. En este trabajo se realizó un analisis semicuantitativo para analizar la expresion de los genes *Med12* en los alelos mutantes y evaluar el efecto de las insersiones en la transcripción del gen. Además, se midieron diferentes rasgos de la arquitectura de la raíz para caracterizar el sistema radicular y la respuesta a fosforo de las mutantes *Zmmed12a* y *Zmmed12b*. Adicionalmente, se investigó la función general de cada uno de los genes con la generación de familias segregantes, diferentes rasgos vegetativos y de floración se evaluaron en plantas adultas en campo; asi como los patrones de segregación. La caracterización molecular de los alelos mutantes mostró que el efecto de las insersiones en el transcrito de *Med12* depende de la localización de la insersion *Ds* o *Mu*. La caracterización fenotípica de la mutantes simples mostró que algunos rasgos relacionados con la adaptación a la respuesta a carencia de fósforo estan activos cuando las mutantes crecen en condiciones suficientes de fósforo, sugiriendo que *Med12* esta involucrado o es necesario para la correcta respuesta de la planta al ambiente. Respecto a las plantas segregantes, el análisis genético mostró que en todas las familias segregantes en diferentes años de siembra se presenta distorsión en la segregación. Debido a la distorsión en la segregación fue dificil recuperar todos los genotipos esperados para realizar un analisis fenotípico completo.

Abstract

Mediator is a muiltiprotein complex highly conserved in all eukaryontes, which functions as either a transcriptional activator or repressor. It regulates different developmental and physiological process, such as developmental timing, organogenesis, hormone responses and the response to abiotic and biotic stress. It is organized into head, middle and tail modules, as well as the additional detachable CDK8 kinase module that consists of MED12, MED13, CDK8 and CYC C. Previous work showed that some miRNAs that respond to phosphate starvation, like miR827, miR397, miR398, are up-regulated in Arabidopsis *med12* mutants grown in optimal phosphate conditions. In addition, approximately 40 miRNAs involved in Root System Architecture (RSA) and morphogenesis, and 11 miRNAs that respond to environmental stress conditions showed expression changes, suggesting an important role of *Med12* in root development and in general, to environmental response. Maize has two paralogous *MED12* genes, named as *ZmMed12a* and *ZmMed12b*, both of which are expressed throughout the plant. In order to investigate the functions of this genes, insertional mutants were generated using *Ac/Ds* and *Mutator* transposon systems. In this work a semi-quantitative analysis was used to analyze the expression of *Med12* genes in the mutant alleles to evaluate the effect of the *Ds* or *Mu* insertions in gene transcription. Different root architectural traits were measured to characterize the root system architecture and the phosphate response of *Zmmed12a* and *Zmmed12b* mutant. In addition, the general function of each gene was investigated with the generation of segregating families, and standard vegetative and flowering traits were evaluated in adult plants grown in the field, as well as the segregation ratios. The molecular characterization of the *Zmmed12a* and *Zmmed12b* mutant alleles showed that the effect of transposon insertions on *Med12* transcripts depends on the location of the *Ds* or *Mu* insertion. The phenotypic characterization of these single mutants showed that some traits related to adaptation to phosphorous response are active when grown in full nutrient conditions, suggesting that *Med12* is involved or is necessary for the correct response to environment. Regarding the *Zmmed12a/+;Zmmed12b/+* segregating plants, genetic analysis showed segregation distortion in all the stocks analyzed and different field years. Due to the segregation distortion it was hard to recover all the genotypic classes to perform a complete phenotypic analysis.

1 Introduction

1.1 Plant responses to the environment

The environment is continually changing, and climate change is expected to cause more extreme variations in weather. Climate change is defined as a change in the statistical distribution of weather patterns for a period of time. It can refer to a change in average weather conditions or in temporal variation of the average long-term conditions, such as in temperature, soil moisture, salinity, ecohydrology, soil fertility, etc. Plants have to respond to their environment in order to grow and reproduce (Ahmad and Prasad, 2012).

Abiotic stresses (e.g. drought, heat, cold, soils with nutrient deficiency) cause a significant reduction in the yield of the major crops around the world. Plant responses to environmental stresses include changes in morphological and structural patterns, as well as in physiological, biochemical and molecular mechanisms that can trigger the process of acclimation or acquisition of tolerance (Potters et al., 2007). At the anatomical level, generic responses include three components: inhibition of cell elongation, localized stimulation of cell division and alterations in cell differentiation. These anatomical changes can be observed mainly in roots, xylem and leaves which contribute to adaptation to unfavorable environmental conditions (Potters et al., 2009, 2007).

Roots are essential for plant adaptation and productivity, as they function in water and nutrient uptake. Root system architecture (RSA) shows high plasticity in response to environmental changes, such as nutrient availability (e.g. low phosphate), soil moisture, temperature, and pH (Khan et al., 2016). RSA refers to the spatial configuration of the root system, and is comprised by primary root length, and the spread, number, and length of lateral roots (Lynch, 1995). Understanding RSA and the mechanisms of its development will allow manipulation and exploitation of different root traits to improve plant adaptation to environmental changes, and increase crop yields (Khan et al., 2016; Lynch, 1995).

Plant abiotic stress responses involve a whole cascade of genes, from stress perception to transcriptional activation of downstream genes, leading to stress adaptation and tolerance

(Ahmad and Prasad, 2012). For this reason, it is important to study the molecular mechanisms by which plants can perceive and integrate environmental signals. The Mediator transcriptional regulatory complex is a key cofactor for integrating different environmental signals with transcription (Buendía-Monreal and Gillmor, 2016; Samanta and Thakur, 2015).

1.2 Plant responses to nutrient deficiency

Water and nutrient availability are the major abiotic stresses that limit plant growth and yield (Lynch, 2011). Plants require a wide range of mineral nutrients in order to carry out the complex processes involved in the biochemical, cellular, physiological and developmental processes underlying growth (Zhang et al., 2014). Phosphorus (P) is an essential macronutrient involved in many processes, such as energy metabolism, cellular signal transduction, biosynthesis of nucleic acids, phospholipids and membranes (Li et al., 2012). However, in approximately 70 % of global cultivated land, the availability of inorganic phosphate (Pi, the form of P that plants can assimilate), is suboptimal, due to high reactivity with cations present in the soil, and immobilization (Li et al., 2012; Lynch, 2011).

Plants have evolved different strategies to optimize P acquisition and internal use, including 1) local Pi sensing and signaling that can initiate modifications of RSA to increase the exploratory capacity and reach Pi-rich patches in the soil, and 2) systemic or long-distance signaling pathways that act to regulate Pi uptake, mobilization and redistribution. Plants can also exude organic acids (OAs) and phosphatases into the soil to release Pi from organic and inorganic sources that are not readily available for plant uptake, and increase the expression of genes encoding high-affinity Pi transporters. Another strategy employed by many plant species is the establishment of symbiotic relations with arbuscular mycorrhizal fungi (Bennetzen and Hake, 2009; Calderón-Vázquez et al., 2011; López-Arredondo et al., 2014). This thesis is focused on the role of the *Med12a* and *Med12b* genes of maize Mediator in regulating root system architecture and the production of phosphatases.

1.2.1 Root system architecture modifications in response to low phosphate

RSA is the result of growth of primary roots, the appearance of secondary roots along primary root axes, the direction of root axis elongation, the senescence or mortality of root axes, and the plasticity of these processes in response to environmental conditions such as soil strength, nutrient availability, water status and oxygen status (Lynch, 1995). The impor-

tance of root architecture in plant productivity results from the fact that many soil resources are unevenly distributed. For example, because of the high adsorption capacity of Pi to soil particles, its mobility is very low, so surface soil layers generally have higher Pi content than subsoil layers. The capacity of plants to find an adequate phosphate supply is directly correlated with their ability to explore the soil. Modifications in root system architecture in response to low Pi are focused on topsoil foraging, where the root system explores the upper part of the soil to allow the exploitation of these Pi reserves (López-Arredondo et al., 2014; Péret et al., 2014).

RSA differs significantly between monocotyledonous and dicotyledonous plants, and between different varieties. In general, however, P starvation causes root trait modifications that tend to increase the exploratory capacity of the plant. Architectural traits associated with enhanced topsoil foraging include shallower growth angles of axial roots, enhanced adventitious rooting, a greater number of axial roots, and greater dispersion of lateral roots (Figure 1.1) (Lynch, 2007). In *Arabidopsis thaliana* and bean (*Phaseolus vulgaris*), P starvation results in a strong reduction in the length of the primary root (PR), modification of root hair growth, changes in root growth angle (RGA) and the diameter and number of lateral roots. Many studies have been conduced to understand the mechanisms underlying these changes in root system architecture, most of them using Arabidopsis as a model (Bonser et al., 1996; Sánchez-Calderón et al., 2006).

In cereals, root modifications in response to low Pi can differ from those observed in Arabidopsis. In rice (*Oryza sativa*) and barley (*Hordeum vulgare*), the effect of low Pi on primary root growth is less pronounced than in Arabidopsis, possibly because their seeds contain more abundant phosphorus reserves (Calderón-Vázquez et al., 2011). In maize, it has been reported that P starvation induces alterations in the postembryonic root system (lateral and crown roots), including modification in the angle, length and number of shoot-borne and lateral roots (Calderón-Vázquez et al., 2009, 2011; Péret et al., 2014). However, the modifications are contrasting to the observed in Arabidopsis. For example, in the inbred line Q319 it was found that the number of lateral roots and lateral root primordia decreased after 6 days of culture in a low phosphate solution, and the primary root growth increase, whereas for Arabidopsis, primary root growth is arrested and lateral roots increase (Li et al., 2012).

Analysis of maize and bean Recombinant Inbred Lines (RILs) varying in root growth angle shows that this trait has a dominant influence on phosphorus acquisition. In bean, phosphorus acquisition and yield rise up to 6-fold and 3-fold (respectively) in low-phosphorus soil, while in maize, phosphorus acquisition increases 2-fold. These observations support a

positive role for RGA in phosphorus acquisition by increasing topsoil foraging (Lynch, 2011; Lynch and Brown, 2001).

Greater adventitious root (AR) formation in some bean genotypes correlates with an increase in growth and phosphorus acquisition in low-phosphorus soil. These benefits may be observed because adventitious roots have shallow RGA and are metabolically cheaper than other root classes. In rice, an induction of adventitious root growth and increases in the number and length of lateral roots are observed (Li et al., 2012; Lynch, 2011). In the case of lateral roots in Arabidopsis, lateral root growth is favored over primary root growth, increasing lateral root elongation and lateral root density.

Root whorl number also increases soil exploration. These underground whorls or nodes emerge from the hypocotyl, with the number varying among genotypes. Roots formed from these whorls in maize are called crown roots, and in bean are basal roots. The first whorls in maize are very short and are located closely together, forming a dense root stock.

Maize crown roots at lower nodes first grow horizontally, and then follow the gravitropic vector. In bean, the uppermost whorls produce roots with shallower RGA, and lower whorls produce roots of progressively steeper angle. In both cases, plants with larger root whorl number could increase soil exploration. In a field study on low phosphorus soil in Mozambique, bean RILs with three whorls accumulated 60 % greater biomass, total root length and leaf area than related RILs with two whorls (Hochholdinger et al., 2004; Lynch, 2011).

Another root adaptive response is the formation of cluster roots. They have been described in white lupin (*Lupinus albus*). Cluster roots are specialized formed by densely spaced lateral rootlets that form at very low Pi conditions and are suppressed at higher Pi supply.

Density of cluster roots is also affected by nitrogen and iron availability. Under phosphorus-limited conditions, they enlarge the surface area of the root for the exudation of large amounts of carboxylates (Neumann et al., 2000).

1.2.2 Plant strategies to release Pi from organic and inorganic sources

Another important strategy for increasing P acquisition from P-limited soils is the release of organic acids and acid phosphatases from roots into the soil. Organic P is not available to plants unless hydrolyzed or mineralized into Pi by phosphatases. The secretion of purple acid

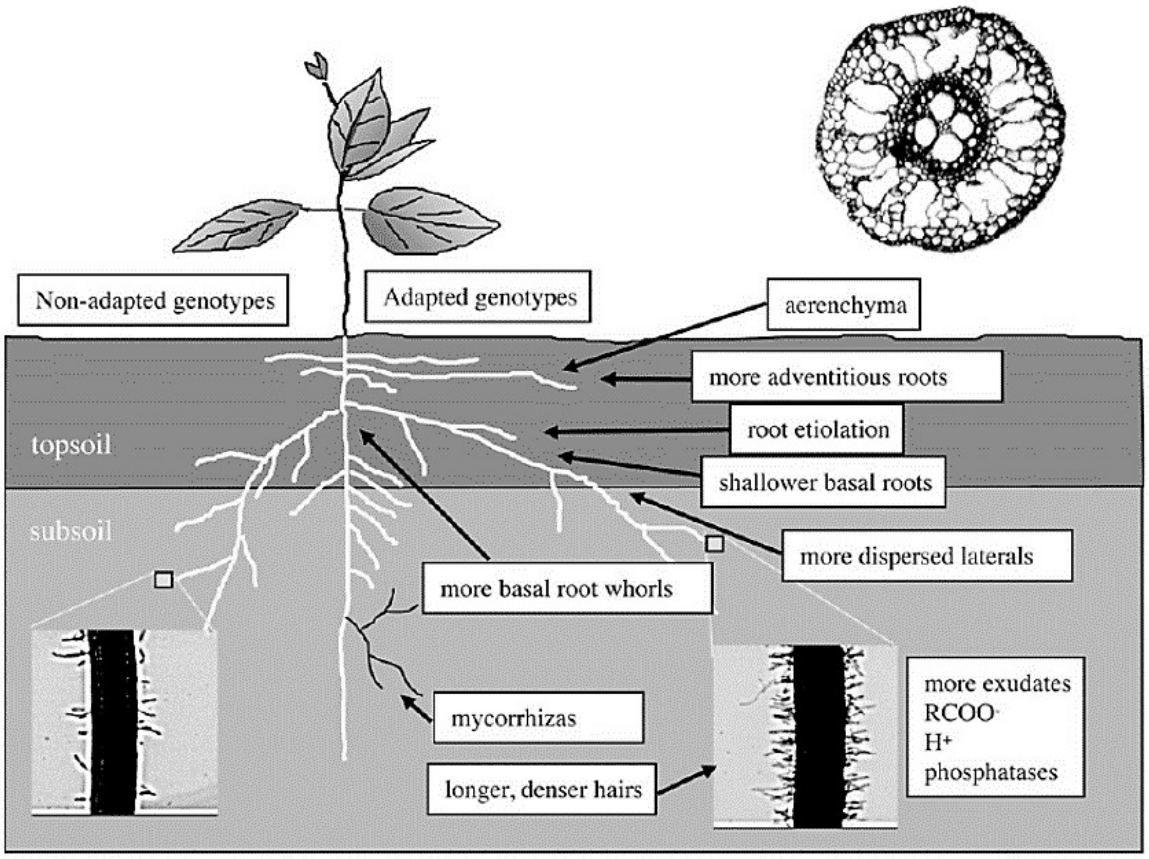

Figure 1.1: **Root phenes associated with genotypic differences in adaptation to low phosphorus. Figure taken from Lynch (2007).**

phosphatase can facilitate utilization of organic P in the rhizosphere (Zhang et al., 2014). Purple acid phosphatases (PAPs) play an important role in P nutrition, both by liberating phosphorus from organic sources in the soil and by modulating distribution within the plant during growth and development. PAPs cleave Pi from ester linkage sites and are relatively stable over wide intervals of pH (4.0–7.6) and temperature (22–60 °F). The importance of PAPs to plant Pi nutrition has been clearly shown through the study of the *pup* (*phosphatase under-producer*) and *atpap10* (*Arabidopsis thaliana purple acid phosphatase 10*) mutants of Arabidopsis, which have reduced purple acid phosphatase activity and display a decreased ability to grow when supplied with organic Pi sources, and through analyses of transgenic plants that overproduce acid phosphatases, which have improved use of organic P sources (González-Muñoz et al., 2015; López-Arredondo et al., 2014).

For these reasons, PAP synthesis and secretion have been important to developing low-Pi tolerance in crops like soybean and common bean. In bean, the level of *PvPAP3* expression was identified as an important trait for low-Pi adaptation, given that its expression

is induced at a higher level in the Pi-efficient genotype G19833 than in the Pi-inefficient genotypes (Liang et al., 2010). In maize, accumulation of transcripts encoding PAPs (e.g. *ZmPAP13, ZmPAP16, ZmPAP30a, ZmPAP10, ZmPAP21c*) was induced in seedling roots and leaves under low P availability (González-Muñoz et al., 2015). In soybean, overexpression of the Arabidopsis *AtPAP15* gene improved Pi availability from organic Pi. These transgenic plants showed improved Pi efficiency and accumulated more dry weight and Pi content than wild-type plants. Also, they produced a larger number of seeds per plant when grown in acidic soil amended with phytate as a Pi source (Wang et al., 2009b).

In the case of organic acids (OA), such as citrate, malate, and oxalate, their production and root exudation enhances Pi availability in Pi-fixing soils. OA exudation is a major trait target for breeding crops with improved Phosphorous Acquisition Efficiency (PAE). Overexpression of citrate synthase and malate dehydrogenase from both microbial and plant origins enhances OA exudation and improves Pi acquisition and plant biomass production in low-Pi soil. Transgenic tobacco lines expressing a mitochondrial malate dehydrogenase gene from the mycorrhizal fungi *Penicillium oxalicum* showed a more than 200 % increase in Pi content and a more than 100 % increase in biomass when grown in aluminum phosphate, iron phosphate, or calcium phosphate (López-Arredondo et al., 2014).

1.2.3 The role of Pi transporters, and transcriptional and microRNA regulation of phosphate starvation responses

Phosphate transporters are critical for P allocation and remobilization within plants, as well as phytohormones (e. g. auxin, ethylene, cytokinins (CKs), abscisic acid (ABA), gibberellins (GA)). Sugars, calcium and microRNAs are also involved in the coordinated response to maintain Pi homeostasis (Chiou and Lin, 2011).
The activity of Pi transporters is regulated by multiple factors and at various steps. General regulation of Pi transport activity has primarily been studied in Arabidopsis. PHT1;1 (AtPT1) and PHT1;4 (AtPT2) contribute predominantly to Pi uptake (Misson et al., 2004). Transcript levels of *PHT1* are positively regulated by PHR1, WRKY75 and sugars, but they are negatively regulated by cytokinin, ABA, MYB62, ZAT6, SPX3, and ARP6/H2A.Z (Devaiah et al., 2009; Karthikeyan et al., 2002; Martín et al., 2000). In addition, PHF1 (PHOSPHATE TRANSPORTER TRAFFIC FACILITATOR1) controls proper trafficking and targeting of PHT1;1 proteins to plasma membranes, and PHO2, a target of miR399, may direct PHT1 protein degradation (Gonzalez et al., 2005). Xylem loading of Pi must be integrated into the process of Pi acquisition, and *PHO1* is indispensable for this activity (Hamburger et al., 2002). PHO1 is transcriptionally suppressed by the direct binding of

WRKY6/42 to its promoter (Chen et al., 2009). Expression of *PHO1* can be activated by sugars and inhibited by cytokinin or ABA (Ribot et al., 2008). It is apparent that sugar and cytokinin act in a contrary fashion to cross-regulate diverse processes of Pi acquisition (Ribot et al., 2008). The transcription factors involved in Pi responses have multiple functions, and are integrated in parallel as well as interconnected pathways consisting of negative or positive regulation (Chiou and Lin, 2011).

In the case of the microRNAs, the best characterized is miR399 and its target *PHO2*. miR399 is up-regulated in low Pi conditions, and directs the cleavage of the *PHO2* mRNA by recognizing the complementary sequences at the 5' UTR (Bari et al., 2006). PHO2 encodes an E2 ubiquitin-conjugating enzyme that controls *PHO1* activity (Liu et al., 2012). The *pho2* mutants of rice and Arabidopsis overaccumulate Pi in their leaves when grown in Pi-sufficient soil, resulting in symptoms of Pi toxicity, and also show the induction of some phosphate starvation-induced genes and phosphate transporters (Delhaize and Randall, 1995; Wang et al., 2009a). Under high Pi conditions, the ubiquitin conjugase activity of *PHO2* promotes *PHO1* degradation (Liu et al., 2012). *PHO1* is a phosphate exporter, and is specifically implicated in the translocation of Pi from the root to shoots by loading Pi into the xylem vessels. In this way, the microRNA miR399 is involved in the maintenance of Pi homeostasis through regulation of PHO2 (Bari et al., 2006; López-Arredondo et al., 2014).

Another well-characterized microRNA that responds to Pi starvation is miR827, which is induced by Pi deprivation to repress its target gene NITROGEN LIMITATION ADAPTATION (NLA). *NLA* encodes a protein containing an N-terminal SPX domain, shown to be responsible for modulation of Pi sensing and uptake in yeast, and a C-terminal RING domain possessing putative ubiquitin E3 ligase activity which its has been reported to regulate the degradation of the PHT1 proteins that modulate Pi transport. *nla* mutants show high Pi accumulation resulting from increases in the levels of several PHT1 proteins (Wei-Yi et al., 2013).

1.3 Mediator complex

Mediator is a multiprotein complex that is conserved in all eukaryotes, acting as a general transcription factor that integrates regulatory signals. from transcription factors bound at gene promoters with changes in Pol II activation. It was discovered in yeast as a complex that contains approximately 20 proteins, and was designated as the Mediator, due to its requirement for transcription of virtually all protein-coding genes (Jing-Wen and Gang, 2014; Kidd et al., 2011). After its discovery in yeast, Mediator was purified from human cells in 1996, and then in 2007 from plant cells (Backstrom et al., 2007; Flanagan et al., 1991; Ito

et al., 1999; Kelleher et al., 1990). Additionally, *in silico* analysis have shown its presence in almost all eukaryotes. Mediator comprises 25 subunits in yeast, approximately 31 subunits in mammals, and approximately 34 subunits in plants. 21 Mediator subunits are conserved between plants other eukaryotes, and six other subunits appear to be plant-specific (Buendía-Monreal and Gillmor, 2016; Kidd et al., 2011).

Structurally, the Mediator complex has been classified into four main modules: the Head, Middle, and Tail as well as the detachable Cyclin Dependent Kinase 8 (CDK8) module (Figure 1.2). Since the active form of Core Mediator (the Head, Middle, and Tail modules) has been purified without the CDK8 module attached and *in vitro* experiments containing the Core Mediator plus CDK8 module cannot maintain transcription activity, the CDK8 module is usually considered as a transcriptional repressor. The CDK8 module is composed of MED12, MED13, CDK8, and its partner Cyclin C (CycC) (Buendía-Monreal and Gillmor, 2016; Kidd et al., 2011).

1.3.1 General role of Mediator

The Head module of Mediator is thought to have the most important initial interactions with RNA pol II, while the Middle module serves a structural function, interacting with RNA pol II once Mediator's conformation changes after its initial interaction with RNA pol II. The Tail module is thought to play an especially important role in interacting with gene-specific transcription factors (Tsai et al., 2014; Robinson et al., 2015). Many Mediator subunits have been functionally characterized, and have been shown to be required in growth and developmental processes (Buendía-Monreal and Gillmor, 2016), as well as environmental responses (Figure 1.2) (Samanta and Thakur, 2015).

1.4 The *Med12* subunit of Mediator influences the phosphate starvation response

Recently, it was found that Arabidopsis *med12* mutants show modifications in root system architecture when grown under phosphate-sufficient as well as in phosphate-deficient conditions. When grown in sufficient phosphate conditions, *med12* seedlings have a shorter primary root and longer root hairs than wt. In low-phosphate, differences observed in primary root length and root hairs were the opposite: *med12* mutants have a longer primary root and root hairs are shorter. *med12* seedlings also showed fewer root hairs in primary and lateral roots in normal phosphate. The fact that root system architecture of *med12* mutants is less affected in low Pi conditions and, that the shoot accumulated less anthocyanins, suggests that *MED12* influences responses to environmental conditions (Martínez-Camacho,

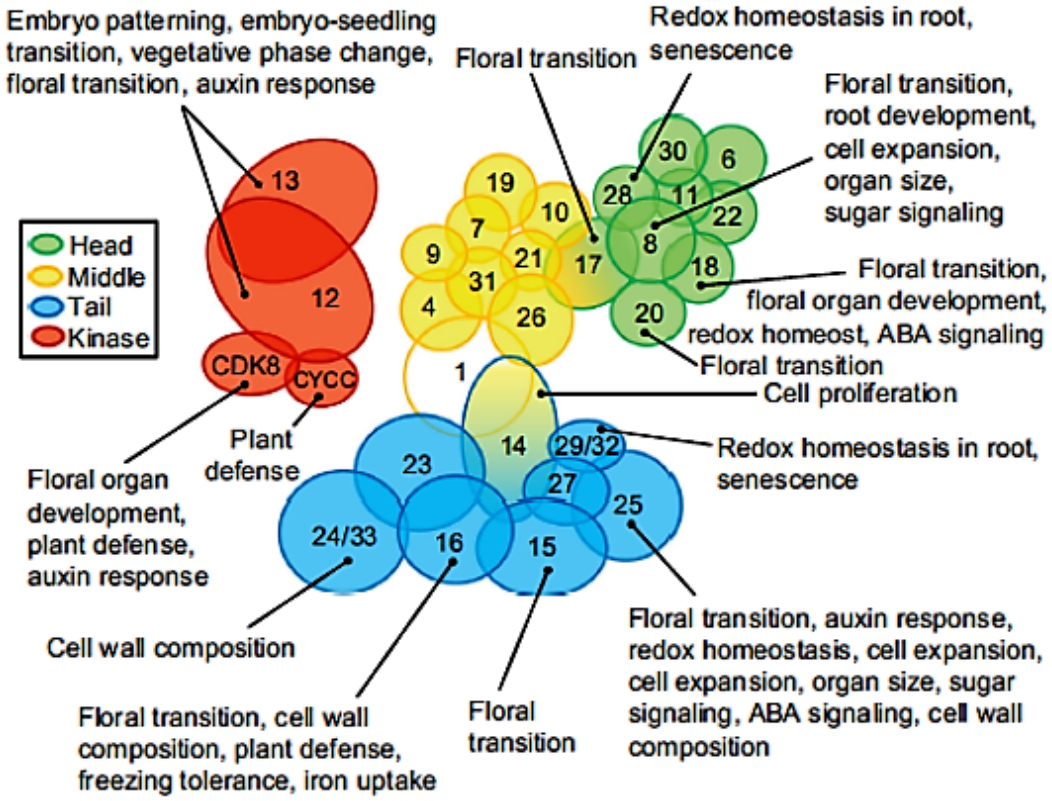

Figure 1.2: **Mediator functions in plant development.** Submodular structure of the plant Mediator complex is depicted on the basis of tridimensional reported structures of yeast Mediator and human Mediator (Robinson et al., 2015; Tsai et al.,2014). Figure taken from Buendía-Monreal and Gillmor (2016).

2015).

The spatio-temporal transcriptional activity of *MED12* was also described. *pMED12::GUS* was expressed throughout vascular tissue. In the shoot, high GUS expression was observed in cotyledon tips, the hypocotyl and stipules; in the roots, *MED12* was expressed in the vasculature of PR and LR. Interestingly, *pMED12::GUS* expression responds to low phosphate conditions, increasing in the root and decreasing in the shoot, in comparison with plants in sufficient phosphate conditions. Also, it was found that the loss of *MED12* results in derepression of some miRNAs that respond to phosphate starvation, for example miR827, which is one of the phosphate-starvation specific miRNAs. miR827 is normally overexpressed only under phosphate starvation stress (Pant et al., 2009). From the above results, coupled with morphological changes in root system architecture, it can be hypothesized that *MED12* is involved in the regulation of phosphate starvation response (Martínez-Camacho, 2015;

Rodríguez-Medina, 2015).

1.5 Maize has two *Med12* genes

Five different genes encode the CDK8 module of Mediator in maize: *Cdk8*, *CycC*, *Med13* and two genes for *Med12*, *ZmMed12a* and *ZmMed12b* (Núñez-Ríos et al., 2017). Med12a and Med12b proteins show 91% protein sequence identity. *Med12a* is located on chromosome 1, and public gene expression data shows that it is constitutively expressed in meristems and vegetative and reproductive organs, is highly expressed during seed development, showing an expression peak in the last stages of endosperm formation and at the mid stage of seed ripening. *Med12b* is located on chromosome 9, and is expressed throughout development, with higher levels during seed formation. In addition, expression of both genes were corroborated experimentally, *ZmMed12a* and *ZmMed12b* are indeed transcribed genes that are expressed in leaves and roots (Núñez-Ríos, 2012). The expression was slightly higher in roots than in leaves, consistent with the eFP browser and public expression data. In summary, according to public expression data, both genes show similar (but not identical) expression patterns (Núñez-Ríos et al., 2017).

The high degree of similarity between *ZmMed12a* and *ZmMed12b* suggests that they are the result of a recent duplication event. *ZmMed12a* and *ZmMed12b* are located in homeologous regions of the genome (1S and 9L, respectively) that derive from a polyploidy event that occurred 5-12 million years ago, sometime after the divergence of maize and sorghum lineages (Núñez-Ríos et al., 2017). Gene duplication raises the possibility for paralog subfunctionalization and consequently, because of mediator role, fine-tuning and improved environmental responses in maize.

In order to investigate the functions of maize *Med12* genes, mutant alleles for each gene were generated. Using a *Ac/Ds* transposon mutagenesis strategy, two mutant alleles from *Med12a* gene were generated. These alleles were designated as *med12a*-1::*Ds* and *med12a*-2::*Ds*, the first one has a *Ds* insertion approximately 900 base pairs before the 5' UTR, and the other one is within exon 10. For *Med12b*, there was a Mu-insertion available in the UniformMu Transposon Resource database. The insertion mu1058248 was confirmed to be inserted in the first exon (Martínez-Camacho, 2015; Núñez-Ríos, 2012).

Based on preliminary results from the *med12* mutant of Arabidopsis, I characterized the root system architecture of the maize *Med12a* and *Med12b* mutants, to determine their role in phosphate starvation responses. In addition, the general function of each gene was investigated with the generation of segregating families, and standard vegetative and flowering

traits were evaluated in adult plants grown in the field.

1.6 Reverse genetics and transposable elements

Reverse genetics starts with a gene whose function is unknown. By analyzing the phenotype of mutations in the gene, the biological function of the gene can be inferred. Generation of mutants can be acheived by chemical mutagenesis, irradiation and insertional methods (Griffiths et al., 2012).

Transposable elements (TE) have been used for mutagenesis in maize since their discovery by Barbara McClintock in 1949. Research on transposable elements began with classical genetic experiments. Remarkably, many of the activities of TEs, such as the ability to transpose, to induce chromosome rearrangements, to undergo cycles of activity and inactivity, and to affect expression of neighboring genes, were described by geneticists long before transposons were molecularly isolated (Peterson, 2013). The three major families of endogenous transposable elements which have been used for gene tagging in maize are *Activator* (*Ac*), *Suppressor-Mutator* (*Spm*) and *Mutator* (*Mu*). These families share common features: they consist of an autonomous element (that requires no other elements for its mobility), and non-autonomous elements (which cannot transpose on their own). Autonomous elements encode the information necessary for their own movement, and for the movement of non-autonomous elements. Because non-autonomous elements do not encode the functions necessary for their own movement, they are stable unless an autonomous element from their family is present somewhere else in the genome (Kunze et al., 1997).

1.6.1 *Ac/Ds* system of transposons

The *Activator* (*Ac*) and *Dissociation* (*Ds*) elements were the first transposons to be discovered. Barbara McClintock observed that chromosome breaks frequently occurred at a specific locus on the short arm of chromosome 9, and chromosome segments occasionally moved to a new location in the genome, so she called this element *Dissociation* (*Ds*). Subsequently she recognized that chromosome breakage and the mobility of *Ds* were dependent on the presence of another locus called *Activator* (*Ac*), that was autonomously able to transpose to new genomic positions (McClintock, 1951).

Ac belongs to the hAT transposon superfamily, along with *hobo* and *Tam3* transposons. All hAT elements have short terminal inverted repeats (11–14 bp in the majority of hAT elements) and generate 8-bp target site duplications upon integration. hAT elements encode

only a single protein, the transposase (TPase), that catalyzes the transposition reaction (Kunze and Starlinger, 1989). The autonomous *Ac* is a small and simple structured transposable element. It is 4,565 bp long, has 11-bp imperfect terminal inverted repeats (TIRs) and approximately 240-bp essential subterminal sequences at both ends, and contains a single gene that encodes the 807 amino acid transposase (TPase). (Lazarow et al., 2013). *Ds* elements are non-autonomous transposons that can be mobilized by the *Ac* TPase, they are a truncated version of the *Ac* element. In contrast to functional and active *Ac* elements, which have been identified in only a few maize lines and in low copy number, hundreds of *Ds* elements are spread throughout the maize genome. The most common *Ds* used in reverse genetics is the *Ds6* element, which carries 1kb of the original autonomous *Ac* element sequence on each end, resulting in a 2kb non-autonomous element (Lazarow et al., 2013).

Ac/Ds elements transpose by a cut-and- paste mechanism. When *Ac/Ds* elements excise, they typically leave behind a "footprint" of additional DNA sequence as a result of target site duplication during insertion. Excision is initiated by single-strand cleavage. Hairpins are generated at the flanking DNA by nucleophilic attack of the exposed 3'-hydroxyl groups to the phosphodiester bonds at the 3'-ends of the transposon DNA leading to the release of the transposon. Hairpins are opened by single-strand cleavage at a variable distance 3' from the nucleotide at the center of the hairpin. The resulting single-stranded 3' overhangs may or may not be exonucleolytically degraded prior to rejoining. After rejoining of the ends and filling-in of the remaining single-stranded gap, the resulting *Ac/Ds* excision footprints carry at the former left and right borders either deletions or palindromic duplications centering around the complementary nucleotide (Lazarow et al., 2013).

1.6.2 *Mutator* system of transposons

The *Mutator* (*Mu*) system, like the *Ac/Ds* system, is broadly used for maize reverse genetics. *Mu* is the most active and mutagenic plant transposon. In lines with active *Mu* transposons, mutation frequencies can exceed the background mutation rate by 50 times, and forward mutation frequencies can be as high as 10^{-3} per locus per generation (Bennetzen, 1996). Because of this property, Mu transposons have been used to generate new mutations in maize with great effect.

The system is regulated by a master autonomous element, *MuDR*, and several non-autonomous elements (*Mu1–Mu13*). All maize *Mu* elements contain conserved 220 bp terminal inverted repeats (TIRs), but each class of element contains unique, apparently unrelated internal sequences. *MuDR* elements contain two genes, *mudrA* and *mudrB*. The best-characterized

mudrA transcript encodes a 120 kDa transposase (MURA); and the major transcript of *mudrB* encodes the 23 kDa protein MURB. The *mudrB* gene is not similar to any sequences outside of maize in any public database and its precise function remains unknown (Lisch, 2002). To understand how this transposon system is regulated, researchers have analyzed Minimal *Mutator* lines. These are lines that carry a very low number of *Mu* elements: as few as a single *MuDR* element and a single non-autonomous *Mu* element inserted into a color gene. Lines carrying a single *MuDR* element have been propagated for many generations without evidence of silencing, a characteristic that has made genetic characterization of *MuDR* in these lines relatively easy. However, a dominant factor was isolated from a Minimal line that, when combined with *MuDR* can cause heritable silencing of one or many *MuDR* elements. This factor, which was designated *Mu killer* (*Muk*), is a rearranged deletion derivative of *MuDR* (Lisch, 2013; Slotkin et al., 2003).

Based on analysis of empty excision sites, somatic *Mu* element excision appears to largely result from non-homologous end joining (NHEJ) of double-stranded gaps, rather than repair from the homologous chromosome. This was supported by the observation that reversion frequency is unaffected if an insertion allele is placed in trans to a deletion or is made homozygous. Coordinate excision and transposition have been directly observed, demonstrating that somatic reversion events are associated with integration. The excision frequency of non-autonomous elements is dependent on the dose of *MuDR*, so two copies of *MuDR* cause roughly twice as many excisions of non-autonomous elements, and a reduced level of activity of a single (or many) *MuDR* element results in a concomitant reduction in excision frequency of those elements. In contrast to somatic events, germinal reversions are extremely rare. The majority of activity in the germline involves transposition without loss of the original element (Lisch, 2002, 2013).

2 Objectives

General objective

Genetic and phenotypic characterization of maize *med12a* and *med12b* mutants.

Specific objectives

1. **Characterization of *Zmmed12a* and *Zmmed12b* single mutants:**
   - Molecular characterization of *Zmmed12a* and *Zmmed12b* mutant alleles.
   - Phenotyping of *Zmmed12a* and *Zmmed12b* single mutants.

2. **Characterization of *Zmmed12a/+;Zmmed12b/+* segregating plants:**
   - Generation of *Zmmed12a/+;Zmmed12b/+* segregating families.
   - Genetic characterization of *Zmmed12a/+;Zmmed12b/+* segregating plants.
   - Phenotyping of *Zmmed12a/+;Zmmed12b/+* segregating plants.

3 Materials and Methods

3.1 Plant material

Different seed stocks were used in this work. For the section of characterization of gene expression in mutant alleles, segregating stocks for each mutant allele were used, RS14-1024.2, RS14-1022 and GH15-61.3 for *Zmmed12a*-1::*Ds*, *Zmmed12a*-2::*Ds* and *Zmmed12b*-1::*Mu*, respectively.

For the phenotypic characterization of single mutants, homozygous stocks for each mutant were used, RS14-1023.2 and RS14-2117.6 for *Zmmed12a* and *Zmmed12b*, respectively. W22 inbred line plants were used as control.

Stocks used to generate families segregating both genes, *Zmmed12a/+;Zmmed12b/+*, are described in section 3.4.

3.2 Analysis of *Med12* gene expression in *Zmmed12a* and *Zmmed12b* mutant alleles

RT-PCR analysis was used to characterize the expression of *Med12* genes in two different *med12a* mutant alleles and one *med12b* mutant allele. Seeds from segregating stocks of each mutant allele were planted. 10 days after germination tissue was collected and genotyped.

Three different homozygous mutant and 3 wild type plants were selected to check gene expression in each allele. RNA was extracted with TRIzol reagent (TermoFisher scientific, cat. 15596018). cDNA was synthesized using the SuperScript III Reverse Transcriptase (Invitrogen, cat. 18080-051) protocol with oligo (dT) primer (for complete protocol see appendix 1).

Two primers sets were used to check *Med12a* expression in *Zmmed12a*-1::*Ds* and *Zmmed12a*-2::*Ds* mutant alleles. One pair to amplify the last fragment of exon 9 (TNC5-TNC4); and the other one amplify a fragment near the 3'UTR (RS167-RS170) (Figure 4.1 A). In the

same way, two primer sets were used to check *Med12b* expression in *Zmmed12b*-1::*Mu*, one pair to amplify the first part of the gene (SG174-SG175), flanking the *Mu* insertion, and the other one amplify a fragment of exon 9 (SG176-SG177) (Figure 4.1 C). The *ZmCDK*, Cyclin-dependent kinase gene (Gene ID: GRMZM2G149286) was used as constitutive gene.

PCR was performed with Kappa Taq DNA polymerase (Kapa Biosystems) under the following cycling conditions: for TNC5-TNC4 primers a touchdown pcr program was used, initial denaturation 95 °C 5 min; 10 cycles of 95 °C 30 sec, 60 °C 30 sec (-0.5 °C per cycle), 72 °C 45 sec; 27 cycles of 95 °C 30 sec, 55 °C 30 sec, 72 °C 45 sec; final extension 72 °C 5 min. For primers RS170-RS167, SG174-SG175, SG176-SG177 and ZmCDK pcr program: initial denaturation 95 °C 5 min; 35 cycles of 95 °C 30 sec, 60 °C 30 sec, 72 °C 2 min; 72 °C 10 min.

3.3 Phenotypic characterization of *Zmmed12a* and *Zmmed12b* single mutants

Phenotypic characterization focused in the root system architecture because previous work showed that the Arabidopsis *med12* mutant was affected in growth and root system architecture (Martínez-Camacho, 2015). To determine if maize mutants were also affected in phosphate responses, 13 plants for each single mutant, *Zmmed12a* and *Zmmed12b*, were planted in sterile sand and watered with Hoagland medium with all the nutrients available. Additionally, plants from parental W22 inbred line were planted as a control.

Plants of 25 day old were harvested and different root architectural traits, root acid phosphatase activity and phosphorous content were measured (for protocols see Appendix 2 and 3). Some traits like root length, crown roots number and crown roots whorls were measured by hand at harvesting, the other ones were measured using root images for each plant and analyzed by DIRT (Digital imaging of root traits), an automatic on line software (http://www.plant-image-analysis.org/software/dirt).

3.4 Generation, genetic characterization and phenotyping of *Zmmed12a/+;Zmmed12b/+* segregating plants

Previous work in our lab found that maize has two paralogs of *Med12* gene (Núñez-Ríos, 2012). An *Ac/Ds* reverse genetic strategy was used to generate mutant alleles of *ZmMed12a* gene; whereas a mutant allele for *ZmMed12b* gene was obtained through the UniformMu Transposon Resource (Martínez-Camacho, 2015; Núñez-Ríos, 2012).

To generate plant families that segregate both genes, crosses between *Zmmed12a* and *Zmmed12b* single mutants were made in the Irapuato field in 2014 (crosses made by Carol Martínez Camacho). Progeny of a cross between *Zmmed12a* (homozygous mutant for gene A) and *Zmmed12b/+* (heterozygous mutant for gene B) (RS14-2119.7 x RS14-2116.5) were planted and genotyped for individual plants carrying both insertions. Positive plants were grown and self-pollinated in the greenhouse and were designated GH15-63. Progeny from GH15-63.4 and GH15-63.6 were planted in the Puerto Vallarta field in 2016. In total 90 kernels were planted. All F2 plants that germinated were genotyped and phenotyped using a field-book app developed by Sherry Flint-García. Some traits were measured during the field season, and others at post harvest (Table 3.1).

3.4.1 Genetic characterization of *Zmmed12a/+*, *Zmmed12b/+* and *Zmed12a/+;Zmmed12b/+* segregating families

To determine if the segregation distortion observed in segregating plants grown in the field was because the number of individuals planted was not enough, 140 individuals from the same seed stocks (GH15-63.4 and GH15-63.6) that had been planted in the Puerto Vallarta field in 2016 were planted in the greenhouse, 10 days after germination, DNA from leaves was extracted and genotyped by PCR.

In addition, the segregation pattern of progeny segregate each gene separately was analyzed. Seeds from RS16-692.3 and RS16-692.13 stocks, segregating only the *ZmMed12a* gene or the *ZmMed12b* gene, were planted in the greenhouse and genotyped by PCR. 100 individual plants for each stock were analyzed.

Finally, in order to confirm if the segregation distortion was still observed in hundreds of progeny, I drastically increased the number of plants analyzed and used different segregating families. 3 different seed stocks segregating only *Zmmed12a/+*, 3 segregating only *Zmmed12b/+* and 10 different seed stocks segregating both genes together, *Zmmed12a/+; Zmmed12b/+*, were selected from progeny obtained in the Puerto Vallarta field in 2016. 90 kernels for each stock were planted in the Puerto Vallarta field in 2017, and the same strategy described above was used to genotype all the plants, for a total of 1320 plants.

To genotype all the plants analyzed in this thesis (e.g. mutant alleles for each gene, segregating plants in the field and in the greenhouse, single mutants in the greenhouse) this general strategy was followed: DNA was extracted from leaves using a rapid extraction protocol (Appendix 4), after the extraction a PCR assay was performed to detect transposon insertion in the plants. Two different primer sets were used to obtain the genotype for each gene, one

primer set was a pair of gene-specific primers to amplify a fragment of the gene flanking the insertion and determine wild-type allele; the other one was a combination of a gene-specific primer and *Ds-* end specific for the *med12a* allele or *Mu-* end specific for the *med12b* allele, to determine mutant alleles. Primers used are listed in appendix 5. Segregation deviating from the expected ratio was determined based on a Chi-square test.

Table 3.1: **Traits measured for phenotyping plants segregating *Zmmed12a/+; Zmmmed12b/+* in the field and post-harvest.**

Phenological traits	**Yield traits**
Germination	Kernel weight
Plants height	Number of kernels per row
Produce ears	Number of rows of kernels
Ear number	Grain rows arrangement
Ear height	Ear shape
Silking	Ear diameter
Tassel length	Ear length
Tassel flowering	
Tassel branches	

4 Results

Characterization of *Zmmed12a* and *Zmmed12b* single mutants:

4.1 Effect of transposon insertions on *ZmMed12a* and *ZmMed12b* transcripts

Maize has two paralogous *Med12* genes, named as *ZmMed12a* (ID: GRMZM2G114459) and *ZmMed12b* (ID: GRMZM5G828278). Both of them are expressed throughout the plant. In order to investigate the functions of these genes, insertional mutants were generated using *Ac/Ds* and *Mutator* transposon systems. For *ZmMed12a*, two mutant alleles were generated using a *Ac/Ds* strategy and were designated as *Zmmed12a*-1::*Ds* and *Zmmed12a*-2::*Ds* (Núñez-Ríos, 2012). In the case of *ZmMed12b*, a Mu-insertion was available in the UniformMu Transposon Resource database. It was requested and analyzed in order to confirm the presence of the Mu-insertion. Individuals carrying the Mu-insertion were propagated and the insertion designated *Zmmed12b*-1::*Mu* (Martínez-Camacho, 2015).

In all three mutant alleles used in this work (2 mutant alleles for *Med12a* and 1 mutant allele for *Med12b*) the presence of transposon insertions was confirmed by PCR. We also wanted to know if these transposon insertions affected *Med12* transcript levels. To investigate this, RT-PCR analysis was used to examine *Med12* transcript accumulation in the three mutant alleles.

To check if *Med12a* gene expression is affected in *med12a*-1::*Ds* and *med12a*-2::*Ds* mutant alleles, two different parts of the gene were analyzed, one in the middle of the gene (using primers TNC5-TNC4) and one near the 3'UTR (using primers RS170-RS167). In *med12a*-1::*Ds* both pairs of primers amplify downstream of *Ds* insertion, while in *med12a*-2::*Ds* one pair ampliflies upstream and the other one downstream of *Ds* insertion (Figure 4.1 A).

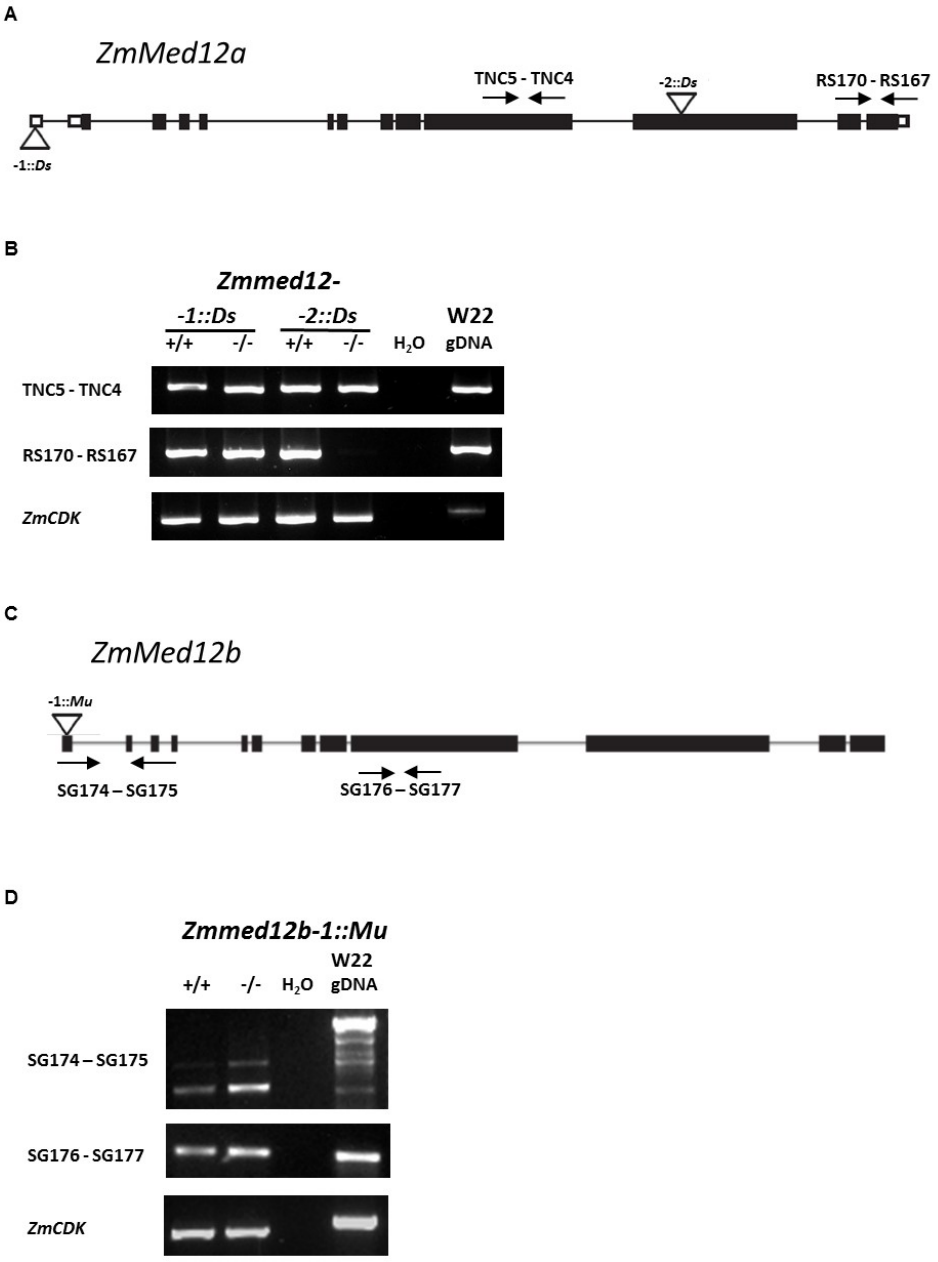

Figure 4.1: **Effect of transposon insertions on *ZmMed12a* and *ZmMed12b* expression.** (A) and (C) *ZmMed12a* and *ZmMed12b* gene structure, respectively, arrow heads indicate the position of the *Ds* or *Mu* insertions of each mutant allele. Arrows show the position of the primers used to check gene expression (Figure modified from Núñez-Ríos et al. (2017)). (B) and (D) RT-PCR expression analysis of *Med12a* and *Med12b* genes, respectively, in 10 day old *Zmmed12a*-1::*Ds*, *Zmmed12a*-2::*Ds* and *Zmmed12b*-1::*Mu* seedlings. +/+ represents a wild type plant, -/- represents a homozygous mutant plant.

In the *med12a*-1::*Ds* mutant allele the *Ds* insertion does not appear to affect the transcription of *Med12a*, since both sections of the gene analyzed are clearly amplified and these sections are downstream of the *Ds* insertion. On the other hand, in the *med12a*-2::*Ds* mutant allele, we found that transcription of *Med12a* upstream of the *Ds* insertion is not affected, but the transcript downstream of the insertion decrease drastically (Figure 4.1 B).

Following the same strategy with *Med12a* gene, two different sections of *Med12b* gene were also analyzed, one flanking the *Mu* insertion (using primers SG174-SG175) and another one downstream (using primers SG176-SG177) (Figure 4.1 C). In both gene sections, the *med12b*-1::*Mu* mutant allele showed transcript, suggesting that the *Mu* insertion has no effects on *Med12b* transcript level (Figure 4.1 D).

4.2 *Zmmed12a* and *Zmmed12b* single mutants show traits associated with adaptation to low phosphorous

It was shown previously that in Arabidopsis *med12* (At4g00450) mutants, root growth and architecture responses to changes in P availability are affected (Martínez-Camacho, 2015). The Arabidopsis *med12* phenotype resembles a phosphate starvation phenotype, showing a shorter principal root and higher lateral root number compared with wild type plants. In addition, an RNA-seq analysis showed that some miRNAs specific to phosphate starvation response are up-regulated in the mutants, suggesting that plant response to phosphate starvation is active (Rodríguez-Medina, 2015). Here, the root system of maize *Zmmed12* single mutants was characterized under non-limiting P conditions.

Phenotypic characterization was performed using the *Zmmed12a*-2::*Ds* mutant allele, because of the clear effect of the *Ds* insertion on *Med12a* transcript levels. In the case of *Med12b*, the *Zmmed12b*-1::*Mu* mutant allele was characterized. After here, I refer to the mutant alleles analyzed, *med12a*-2::*Ds* and *med12b*-1::*Mu* as *Zmmed12a* and *Zmmed12b* single mutants.

In general, the *Zmmed12a* and *Zmmed12b* mutants showed different phenotypes between them at 25 days after germination (Figure 4.2 A). However, only some of the traits measured showed a significant differences between the two mutants (Table 4.1). W22 plants are significantly different from *Zmmed12b* for almost all traits, but there are not many differences between W22 and *Zmmed12a* mutants.

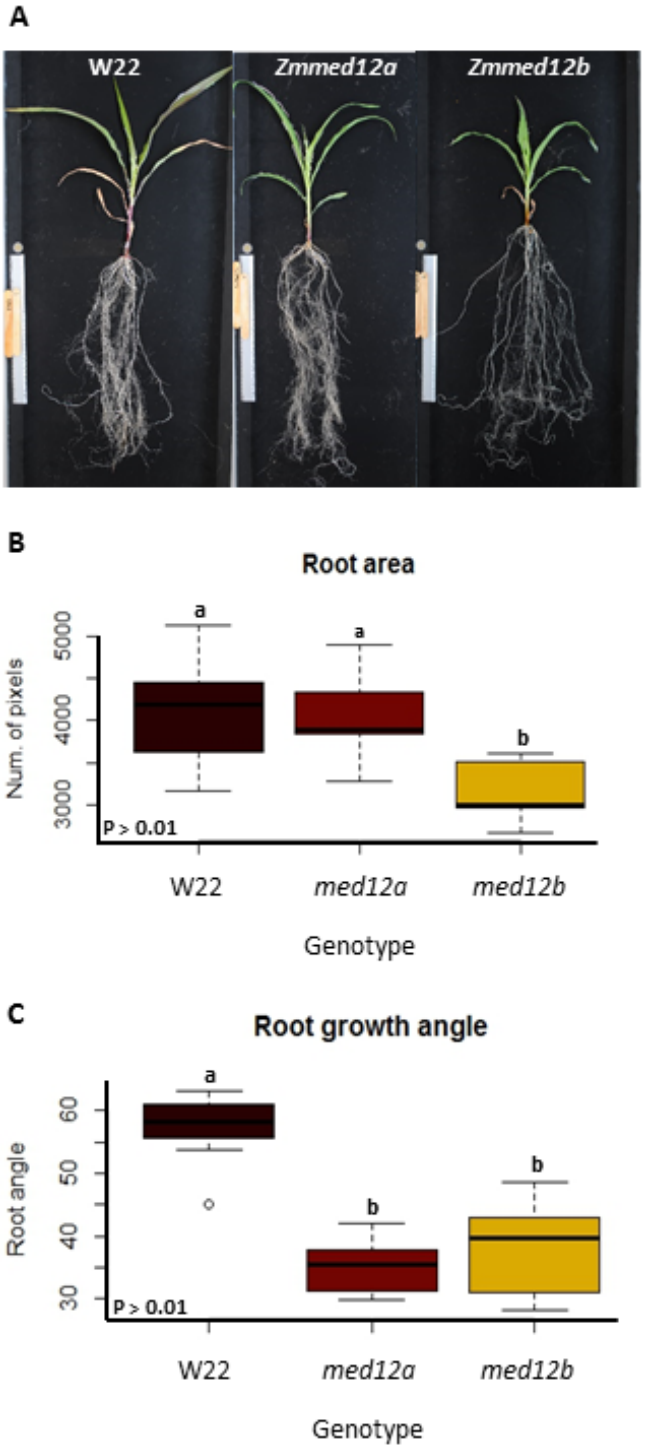

Figure 4.2: **Root phenotypic characterization of *Zmmed12a* and *Zmmed12b* single mutants.** (A) General overview of *Zmmed12a*, *Zmmed12b* and W22. 25 day old plants, grown in sterile sand with all nutrients available. Roots images were taken from 13 different plants from each genotype, and were analyzed using DIRT. (B) Root area, projected root area is represented by the number of pixels belonging to the root in the image. (C) Root growth angle, root top angle measured with respect to position of the soil. Different letters indicate significant differences between genotypes. A Tukey honest significant difference (HSD) test was used to determine significant differences ($P \leq 0.01$).

Table 4.1: **Root architecture traits measured in *Zmmed12a* and *Zmmed12b* single mutants grown in optimal phosphate conditions.**

Trait	Genotype W22	*Zmmed12a*	*Zmmed12b*
Total root length (cm)	56.3 ± 9.9	67.7 ± 12.5	56 ± 15.8
Crown root number	11.9 ± 1.9^a	9.5 ± 1.3^b	8.6 ± 1.9^b
Crown root whorls	2.7 ± 0.4	2.4 ± 0.5	2.5 ± 0.5
Root growth angle	48.7 ± 6.5^a	33.3 ± 11.7^b	38.6 ± 8.2^b
Root area[1]	4113 ± 534^a	4115 ± 597^a	2884 ± 744^b
Stem diameter	7.6 ± 1	8.4 ± 0.5	6.9 ± 0.9
Root density[2]	1.73 ± 0.4	1.5 ± 0.3	1.2 ± 0.5
Root tip number[3]	139.7 ± 31.2^a	108.1 ± 19.6^a	58.6 ± 19.4^b
Root tip diameter[4]	0.5 ± 0.008^a	0.53 ± 0.01^a	0.61 ± 0.02^b
Biomass[5]			
Shoot	0.68 ± 0.09^a	0.55 ± 0.06^a	0.35 ± 0.1^b
Root	0.7 ± 0.18	0.79 ± 0.09	0.62 ± 0.2
Total	1.4 ± 0.28	1.28 ± 0.15	0.98 ± 0.3

Measurements shows the mean of 13 different plants for each genotype. Plants were grown in sterile sand with all nutrients available, harvested and measured after 25 days after germination.
[1] Projected root area is represented by the number of pixels belonging to the root.
[2] Average root density is represented by the ratio foreground to background pixels with in the root shape.
[3] Number of root tip corresponds to the overall number of tips detected in the image.
[4] Mean tip diameter is estimated from the medial circle overall detected tips.
[5] Biomass is represented in grams of dry weight.
[a,b] Letters indicate significant differences between genotypes. A Tukey honest significant difference (HSD) test was used to determine significant differences ($P \leq 0.05$).

Biomass is the most evident difference between the mutants, since *Zmmed12a* looks bigger than *Zmmed12b*. The aerial part and stem diameter of *Zmmed12a* are clearly bigger than *Zmmed12b*, but in the case of the root biomass, there are no differences between them. Interestingly, the root area and number of root tips are larger in *Zmmed12a* than in the *Zmmed12b* mutant (Figure 4.2, Table 4.1).

Other root architectural traits measured (crown root number, crown root whorls, root density and total length) were not significantly different between genotypes (Table 4.1).

Both mutants have shallower roots than W22 plants, meaning that mutant roots grow superficially (Figure 4.2 C), a response potentially related to growth under low P. Another trait related with adaptation to low P is production of acid phosphatases. This trait was measured in roots, and it was found that in *Zmmed12b* mutants the phosphatase activity is higher compared with *Zmmed12a* and W22 (Figure 4.3 A).

Phosphorous (P) content was also quantified in both single mutants and W22 plants. It was found that the P concentration is different between the mutants and wild type plants. *Zmmed12a* mutants show greater P concentration in roots than *Zmmed12b* and W22, while *Zmmed12b* presents increased P concentration in shoots in comparison with *Zmmed12a* and W22. The root-shoot P relation in *Zmmed12a* and *Zmmed12b* is different, compared with W22. For *Zmmed12a*, P concentration is a little bit higher in roots than in the shoot. In the case of *Zmmed12b*, P concentration in shoot is almost the double than in roots (Figure 4.3 B).

Characterization of *Zmmed12a/+;Zmmed12b/+* segregating plants:

4.3 Generation of *Zmmed12a/+;Zmmed12b/+* segregating families

As described above, maize has two *Med12* paralogs and single mutants for each gene were generated using different transposon systems (Martínez-Camacho, 2015; Núñez-Ríos, 2012). Using these single mutants, different segregating families were generated to allow phenotypic analysis of double and single mutant combinations. Comparing phenotypes within segregating families avoids effects due to any differences that might arise in lines that were developed and maintained independently. Additionally, using segregating stocks allows determination of the function of each *Med12* gene, and any interaction between them.

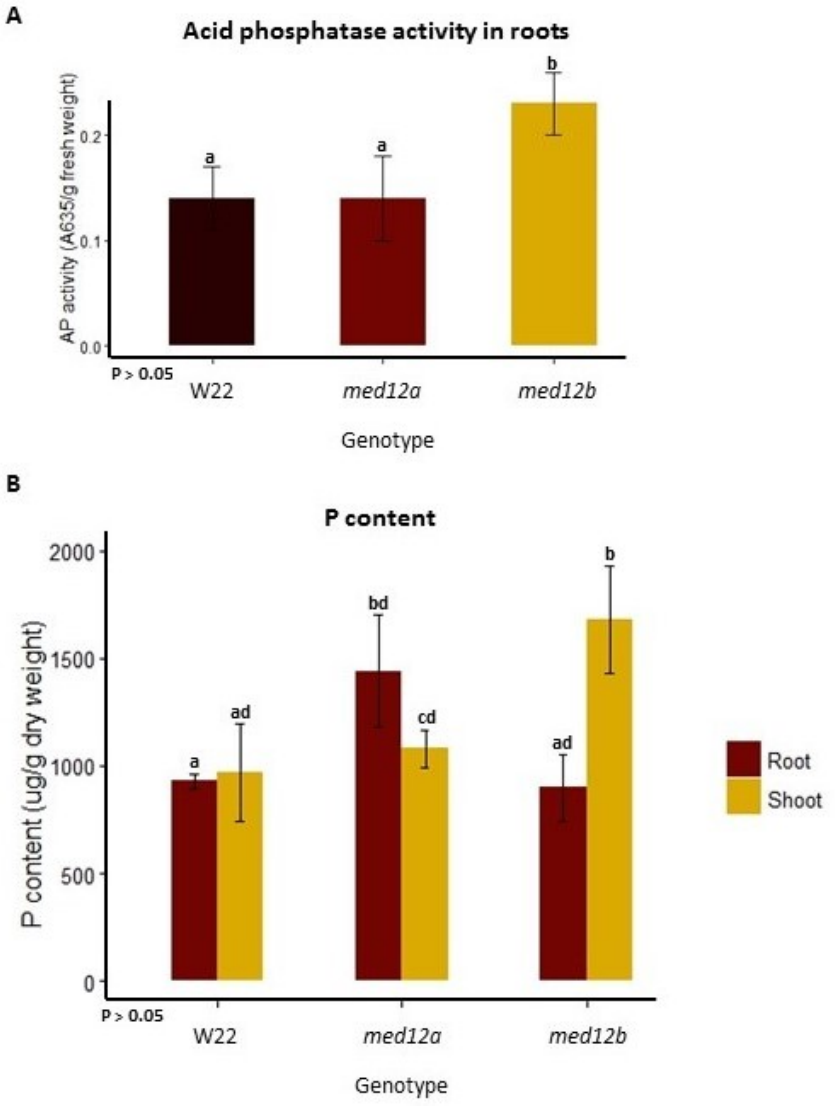

Figure 4.3: **Acid phosphatase activity and phosphate content in *Zmmed12a* and *Zmmed12b* single mutants present changes in optimal phosphorous conditions.** Plants from each genotype were grown in optimal phosphorous conditions and harvested 25 days after germination to measure (A) acid phosphatase activity in roots and (B) phosphorous content in shoots and roots. Six different plants for each genotype were used. Different letters indicate significant differences between genotypes and/or tissues. A Tukey honest significant difference (HSD) test was used to determine significant differences ($P \leq 0.05$).

A single F1 family that came from a cross between *Zmmed12a* (homozygous mutant for gene A) and *Zmmed12b/+* (heterozygous for gene B) was selected for further analysis because of its high percentage of germination. These F1 stock was generated in the summer of 2014 by Carol Martínez. About 50 kernels from this stock were genotyped to look for plants with both the *Ds* insertion in *ZmMed12a* gene and the *Mu* insertion in *ZmMed12b*. Genotyping

was performed looking for plants that carry the *Mu* insertion, since the *med12b* parent was heterozygous for the insertion, while the *med12a* parent was homozygous.

Five different plants from the 50 genotyped kernels had both insertions. These 5 plants were grown and self-pollinated in the greenhouse, and were designated as GH15-63. Progeny of two different plants, GH15-63.4 and GH15-63.6, were planted in Puerto Vallarta field in 2016. In total 90 kernels were planted in the field and 66 germinated. All of them were genotyped by PCR and subsequently phenotyped.

A number of the 66 plants that were grown in the field in 2016 were self-pollinated, and 44 ears were harvested at the end of the season. Progeny of these ears were used to investigate the segregation pattern of plants that segregate only one gene. The plants were germinated in the greenhouse and genotyped 10 days after germination.

In addition, from the 44 new stocks generated in 2016, 3 different stocks that segregate only *Zmmed12a*, 3 that segregate only *Zmmed12b* and 10 different stocks that segregate both genes together *Zmmed12a;Zmmed12b* were planted in the field in 2017. 90 kernels for each of these 16 stocks were planted. In total, 1320 plants germinated, and all of them were genotyped and phenotyped in the field in the same way as the previous year.

4.4 *Zmmed12a/+;Zmmed12b/+*, *Zmmed12a/+* and *Zmmed12b/+* segregating plants show segregation distortion

For this thesis, segregation pattern data of *Zmmed12a* and *Zmmed12b* mutants was obtained from two different field years and one greenhouse experiment. Results are presented in chronological order.

Zmmed12a/+;Zmmed12b/+ plants grown in the Puerto Vallarta field in 2016

Five *Zmmed12a/+;Zmmed12b/+* segregating families were generated, and progeny of two of these five families were planted in the field in 2016. 66 plants germinated, tissue from leaves was collected, and all plants were genotyped by PCR. After genotyping, it was found that there was segregation distortion in the plants grown in the field. Six of nine genotypic classes expected were found from this F2. Surprisingly, *Zmmed12a* homozygous mutants were absent, and also from all genotypic classes (Table 4.2). Segregation of each gene was analyzed also independently (Table 4.3).

Table 4.2: **Segregation ratios of *Zmmed12a/+;Zmmed12b/+* plants grown in the 2016 field.**

Genotypes[a]	**Expected**	**Observed**	X^2 **value**	**P-value***
AA;BB	4.1	1	51.8	1.825e-08
AA;Bb	8.3	13		
Aa;BB	8.3	6		
Aa;Bb	16.5	38		
AA;bb	4.1	3		
aa;BB	4.1	0		
Aa;bb	8.3	5		
aa;Bb	8.3	0		
aa;bb	4.1	0		

[a]Genotypes are represented by letters A and B, for *Med12a* and *Med12b* genes, respectively.
∗Critical value of the X^2 distribution.
Capital letters denominate the wild type allele.
Lower case letters denominate the mutant allele.

Table 4.3: **Segregation ratios of *Zmmed12a* and *Zmmed12b* alleles, analyzed separately. Segregating plants grown in the 2016 field.**

Genotypes[a]	**Expected**	**Observed**	X^2 **value**	**P-value***
AA	16.5	17	24.27	5.361e-06
Aa	33	49		
aa	16.5	0		
BB	16	6	20.37	3.764e-05
Bb	33	50		
bb	16	8		

[a]Genotypes are represented by letters A and B, for *Med12a* and *Med12b* genes, respectively.
∗Critical value of the X^2 distribution.
Capital letters denominate the wild type allele.
Lower case letters denominate the mutant allele.

.

If each gene is analyzed independently, from the progeny of a self-pollinated heterozygous plant, we expect three different genotypes. The analysis of each gene independently, can show us in a simple way if the segregation distortion observed is present even if all the genotypes expected are observed, at least for *Zmmed12b* allele. In the case of *ZmMed12a* gene, segregation distortion is also present because, no homozygous mutant for this gene were found. Nevertheless, it was observed that the heterozygous number is a little bit higher

than expected. For *ZmMed12b* gene all the genotypes are present, the number of wild-types and homozygous mutants is less that the expected and heterozygous plants, like *ZmMed12a*, are over represented (Table 4.2).

Segregation ratios of *Zmmed12a/+*, *Zmmed12b/+* and *Zmmed12a/+; Zmmed12b/+* plants analyzed in the greenhouse

In order to know if the segregation distortion observed in the plants grown in the field is due to the small number of plants analyzed or because there is an interaction between the genes, segregation ratios of plants segregating each gene independently (single mutants) and plants segregating both genes were analyzed. Plants were germinated in the greenhouse and were genotyped 10 days after germination. For the single mutants, two stocks obtained in the 2016 field were used, and 100 individuals for each gene were genotyped. For plants segregating both genes, 140 individuals were genotyped from the same two stocks planted in Puerto Vallarta in 2016 (GH15-63.4 and GH15-63.6).

All genotypic classes expected from the segregating families grown in the greenhouse were found, but the segregation ratios were not as expected. In the case of plants that segregate only *Zmmed12a*, three important things were found. First, homozygous mutants for this gene are present, suggesting that they are not viable when grown in the field but are in the greenhouse. Second, only less than half the expected number of this homozygous mutants were found. Third, wild type and heterozygous classes have the same behavior as the plants in the field: the number of wild type plants was as expected, and the number of heterozygous was higher than expected (Table 4.4). For plants segregating *Zmmed12b*, the same behavior as in the field were found: less wild type and homozygous mutants and over representation of the heterozygous class (Table 4.5).

Analyzing the segregation ratios from the family segregating both genes grown in the greenhouse, it was possible to verify some important points: 1.- Homozygous mutant plants for both genes, *Zmmed12a;Zmmed12b*, are viable in the greenhouse and, 2.- Segregation distortion is observed, even when increasing the number of plants and even when all the nine genotypic classes expected were recovered (Table 4.6).

Segregation ratios observed in these plants are more or less the same as that observed in the 2016 field. The wild type class is the only one that shows a number of individuals closer to expected. All the classes that have a homozygous mutant allele showed fewer individuals than expected. In particular, single mutants and double homozygous mutants, show half or less individuals than the expected. In the case of heterozygous classes, all of them show more

individuals than expected: heterozygous plants for both genes are the highest genotypic class (Table 4.6).

Segregating plants grown in the greenhouse came from the same stocks as plants grown in the 2016 field. To confirm that segregation distortion remains, even when increasing the number of plants, segregation ratios obtained in both experiments were added and analyzed for each individual gene. More than 200 individuals were analyzed, segregation ratios for *Zmmed12a* and *Zmmed12b* showed segregation distortion, in agreement with previous analysis. Homozygous mutants are almost half less than expected, and it is clear that the heterozygous class is over represented in both cases (Table 4.7).

Table 4.4: **Segregation ratios of plants segregating only *Zmmed12a* allele grown in the greenhouse.**

Genotypes[a]	**Expected**	**Observed**	X^2 **value**	**P-value***
AA	25.25	28	9.43	0.0089
Aa	50.5	61		
aa	25.25	12		

[a]Genotypes are represented by letters A for *Med12a* gene.
∗Critical value of the X^2 distribution.
Capital letters denominate the wild type allele.
Lower case letters denominate the mutant allele.

Table 4.5: **Segregation ratios of plants segregating only *Zmmed12b* allele grown in the greenhouse.**

Genotypes[a]	**Expected**	**Observed**	X^2 **value**	**P-value ***
BB	24.25	9	23.78	6.847e-06
Bb	48.5	72		
bb	24.25	16		

[a]Genotypes are represented by letters B for *Med12b* gene.
∗Critical value of the X^2 distribution.
Capital letters denominate wild type allele.
Lower case letters denominate the mutant allele.

.

Table 4.6: **Segregation ratios of *Zmmed12a/+;Zmmed12b/+* plants grown in the greenhouse.**

Genotypes[a]	**Expected**	**Observed**	X^2 **value**	**P-value***
AA;BB	8.8	10	21.9	0.005077
AA;Bb	17.5	24		
Aa;BB	17.5	24		
Aa;Bb	35	47		
AA;bb	8.8	2		
aa;BB	8.8	6		
Aa;bb	17.5	12		
aa;Bb	17.5	11		
aa;bb	8.8	4		

[a]Genotypes are represented by letters A and B, for *Med12a* and *Med12b* genes, respectively.
∗Critical value of the X^2 distribution.
Capital letters denominate wild type allele.
Lower case letters denominate the mutant allele.

Table 4.7: **Summary of segregation ratios of *Zmmed12a/+;Zmmed12b/+* plants grown in the field in 2016 and in the greenhouse, analyzed by gene.**

Genotypes[a]	**Expected**	**Observed**	X^2 **value**	**P-value***
AA	51	49	29.59	3.74e-07
Aa	102	135		
aa	51	20		
BB	53.5	43	32.67	8.05e-08
Bb	107	137		
bb	53.5	20		

[a]Genotypes are represented by letters A and B, for *Med12a* and *Med12b* genes, respectively.
∗Critical value of the X^2 distribution.
Capital letters denominate wild type allele.
Lower case letters denominate the mutant allele.

Segregation ratios of *Zmmed12a/+*, *Zmmed12b/+* and *Zmmed12a/+; Zmmed12b/+* segregating plants grown in the 2017 field

Some plants that germinated in the field in 2016 were self-pollinated, and 44 new stocks were generated. From these stocks generated in the field, 3 different stocks that segregated only *Zmmed12a*, 3 segregating only *Zmmed12b* and 10 stocks segregating both genes together *Zmmed12a;Zmmed12b* were planted in the field in 2017. Different seed stocks were analyzed, to investigate if the segregation distortion observed in the 2016 field and in the greenhouse experiment was observed in multiple stocks.

90 kernels for each stock were planted, and the percentage of germination was very good, above 91% in *Zmmed12a/+* and *Zmmed12a/+;Zmmed12b/+* stocks, and above 85% in *Zmmed12b/+*. In total, 1320 plants germinated: 247, 244 and 851 that segregated *Zmmed12a*, *Zmmed12b* and *Zmmed12a;Zmmed12b*, respectively. Almost all of them were genotyped by PCR.

After genotyping, segregation ratios of each family were analyzed. Segregation ratios of *Zmmed12a/+* and *Zmmed12b/+* are very similar. Both genes show segregation distortion in all the stocks analyzed. Combined data from the three different stocks used for gene A and gene B are shown in table 4.8 and 4.9, respectively. For *Zmmed12a/+*, 159 plants were genotyped, and, for *Zmmed12b/+*, 124 plants were genotyped. Surprisingly, the number of wild type plants, for both genes, is very high, at least three times that expected. Conversely, the number of heterozygous and homozygous mutants is very low compared to expected. In the case of *Zmmed12a/+*, heterozygous plants are about half the number expected, and again no homozygous mutants for *ZmMed12a* were found, like in the 2016 field (Tables 4.8 and 4.9).

Table 4.8: **Segregation ratios of plants segregating only *Zmmed12a* allele grown in the 2017 field.**

Genotypes[a]	Expected	Observed	X^2 value	P-value*
AA	39.75	122	232.66	2.2e-16
Aa	79.5	37		
aa	39.75	0		

[a]Genotypes are represented by letters A for *Med12a* gene.
∗Critical value of the X^2 distribution.
Capital letters denominate wild type allele.
Lower case letters denominate the mutant allele.

Table 4.9: **Segregation ratios of plants segregating only *Zmmed12b* allele grown in the 2017 field.**

Genotypes[a]	**Expected**	**Observed**	**X^2 value**	**P-value***
BB	31	112	282.24	2.2e-16
Bb	62	7		
bb	31	5		

[a]Genotypes are represented by letters B for *Med12b* gene.
∗Critical value of the X^2 distribution.
Capital letters denominate wild type allele.
Lower case letters denominate the mutant allele.

Table 4.10: **Segregation ratios of *Zmmed12a/+;Zmmed12b/+* plants grown in the 2017 field.**

Genotypes[a]	**Expected**	**Observed**	**X^2 value**	**P-value***
AA;BB	20.9	54	231.53	2.2e-16
AA;Bb	41.8	62		
Aa;BB	41.8	97		
Aa;Bb	83.7	93		
AA;bb	20.9	1		
aa;BB	20.9	6		
Aa;bb	41.8	6		
aa;Bb	41.8	14		
aa;bb	20.9	2		

[a]Genotypes are represented by letters A and B, for *Med12a* and *Med12b* genes, respectively.
∗Critical value of the X^2 distribution.
Capital letters denominate wild type allele.
Lower case letters denominate the mutant allele.

.

10 different stocks segregating both genes together were analyzed. For all stocks, segregation distortion was detected, out of a total of about 400 plants. All 9 genotypic classes expected were found, including the double homozygous mutant. However, the number of single homozygous mutants was very low compared to expected. Also, genotypic classes that are homozygous mutant for either of the two genes, are less prevalent. For the heterozygous classes, a higher number of individuals than expected was found (Table 4.10).

Finally, when each gene of these *Zmmed12a/+;Zmmed12b/+* segregating families was analyzed independently, segregation distortion is clearly observed and is in agreement with that observed in the 2016 field and with the greenhouse experiment. In general, there is over representation of heterozygous plants, very few homozygous mutants are present and wild type plants are closer to the expected numbers (Table 4.11). With these numbers, we can confirm that the segregation distortion observed is not because of a low number of plants analyzed, and is also not a effect found in a single family.

Table 4.11: **Segregation ratios of *Zmmed12a/+;Zmmed12b/+* plants grown in the 2017 field, analyzed by gene.**

Genotypes[a]	**Expected**	**Observed**	X^2 **value**	**P-value***
AA	97.7	79	77.85	2.2e-16
Aa	195.5	277		
aa	97.7	35		
BB	89.7	99	102.09	2.2e-16
Bb	179.5	251		
bb	89.7	9		

[a]Genotypes are represented by letters A and B, for *Med12a* and *Med12b* genes, respectively.
∗Critical value of the X^2 distribution.
Capital letters denominate wild type allele.
Lower case letters denominate the mutant allele.

4.5 Phenotyping of *Zmmed12a/+;Zmmed12b/+* segregating plants grown in the 2016 field

Plants from two *Zmmed12a/+;Zmmed12b/+* segregating families were planted in the Puerto Vallarta field in 2016. In total, 66 plants germinated and were phenotyped using the field book app developed by Dr. Sherry Flint-Garcia. Some traits were measured during plant growth and others after harvesting (Table 3.1).

All 66 plants that germinated in the 2016 field were genotyped. After genotyping, 6 of 9 genotypic classes expected from a F2 segregating two genes were observed. The wild type class was represented by a single plant (Table 4.2). To use this wild type phenotype as a reference and make comparisons with statistical significance with other genotypic classes, phenotypic data from 10 W22 inbred line plants that grew in the same field were used as external control. Both *med12* mutants are in the W22 background.

Plants segregating *Zmmed12a;Zmmed12b* showed 74% germination in the 2016 field. All the plants that germinated develop normally during their life cycle, and were able to produce ears and tassel. The average ear production was 2 ears per plant, no matter the genotypic class (Table 4.12).

Other traits like plant height, ear diameter, ear and tassel length did not show significant differences between the genotypic classes, but plants heterozygous for *Zmmed12a* and homozygous mutant for *Zmmed12b* (Aa;bb) tended to be shorter than the other genotypes (Table 4.12).

Flowering time is a very important trait for yield: in the case of maize it is very important to evaluate the synchronization of pollen shed and silking. For this reason, this trait was analyzed in detail in the segregating plants. It was also of particular interest because Arabidopsis *med12* mutants are delayed in flowering time (Gillmor et al., 2014). The Anthesis-Silking Interval (ASI) was calculated for every genotypic class. ASI measures the time between pollen shed and silking, where smaller values mean that successful pollination events increase. *Zmmed12a/+;Zmmed12b/+* segregating plants presented small ASI values (in most of the plants the silks were ready before anthesis), indicating a correct synchronization between the pollen shed and silking (Figure 4.4 A).

Finally, yield of *Zmmed12a/+;Zmmed12b/+* segregating plants was analyzed. Non-significant differences were found in the yield between the six genotypic classes. But when the weight of 50 kernels per ear was compared, interesting differences were found (Figure 4.4 B). The weight of 50 kernels per ear represents seed size. Average seed size for the wild type genotypic class was 10.9 g (W22), although it was not statistically different from the other five classes. Heterozygous (AA;Bb) and homozygous (AA;bb) mutant plants for *Zmmed12b* may have bigger seeds than wt plants, and also than the other genotypes (Figure 4.4 B). The absence of *Med12b* gene increase the seed size, but only when plants are wild type for *Med12a* gene. This is evident in the homozygous *Zmmed12b*; heterozygous *Zmmed12a* mutant plants (Aa;bb) when the seed weight decrease to 8.7 g. In the case of double heterozygous (Aa;Bb) is not very clear because this class shows a lot of variation (Figure 4.4).

If the number of mutant alleles is observed it can be suggested that each gene contributes in a different way and the effect depends on the allele combination. Further work with all the genotypic classes is necessary to try to confirm and better understand the interaction between both genes.

Table 4.12: **Traits measured when phenotyping *Zmmed12a/+;Zmmed12b/+* segregating plants grown in Puerto Vallarta field in 2016.**

Genotypes*	Mutant alleles**	Plant height	Ear number	Ear diameter	Ear length	Rows of kernels	Tassel branches	Tassel length
W22 (10) •	0	128 ± 5	1.3 ± 0.5	3.58 ± 0.08	9.2 ± 0.5^{a}	13.5 ± 0.9	NA	NA
AA;BB (1)	0	145	2	2.9	10.4	14	8	31.2
AA;Bb (13)	1	135.9 ± 7	1.7 ± 0.4	3.5 ± 0.3	11.7 ± 1.2^{b}	14.9 ± 1.3	7.8 ± 2.1	30.4 ± 2.7
Aa;BB (6)	1	127.5 ± 10.4	2 ± 0	3.4 ± 0.11	10.8 ± 1.7	15.2 ± 1.5	9 ± 2	30.2 ± 1.5
Aa;Bb (38)	2	126.6 ± 21.4	1.8 ± 0.5	3.5 ± 0.3	11.3 ± 1.4^{b}	14.7 ± 1.5	7 ± 2	30.3 ± 4.5
AA;bb (3)	2	130 ± 21	1.6 ± 0.5	3.6 ± 0.15	11.2 ± 0.4	14 ± 0	7.3 ± 3.2	31 ± 0
Aa;bb (5)	3	115.2 ± 20.5	2 ± 0	3.58 ± 0.1	11.4 ± 3.1	14 ± 0	7.2 ± 2.9	28.7 ± 2.7

*Genotypes are represented by letters A and B, for *Med12a* and *Med12b* genes, respectively.
• Number into parenthesis indicate number of plants for each genotypic class.
∗ ∗ This is the sum of mutant alleles for genotype.
NA no measurement.
Capital letters denominate the wild type allele.
Lower case letters denominate the mutant allele.
^{a,b} Letters indicate significant differences between genotypes. A Tukey honest significant difference (HSD) test was used to determine significant differences ($P \leq 0.05$).

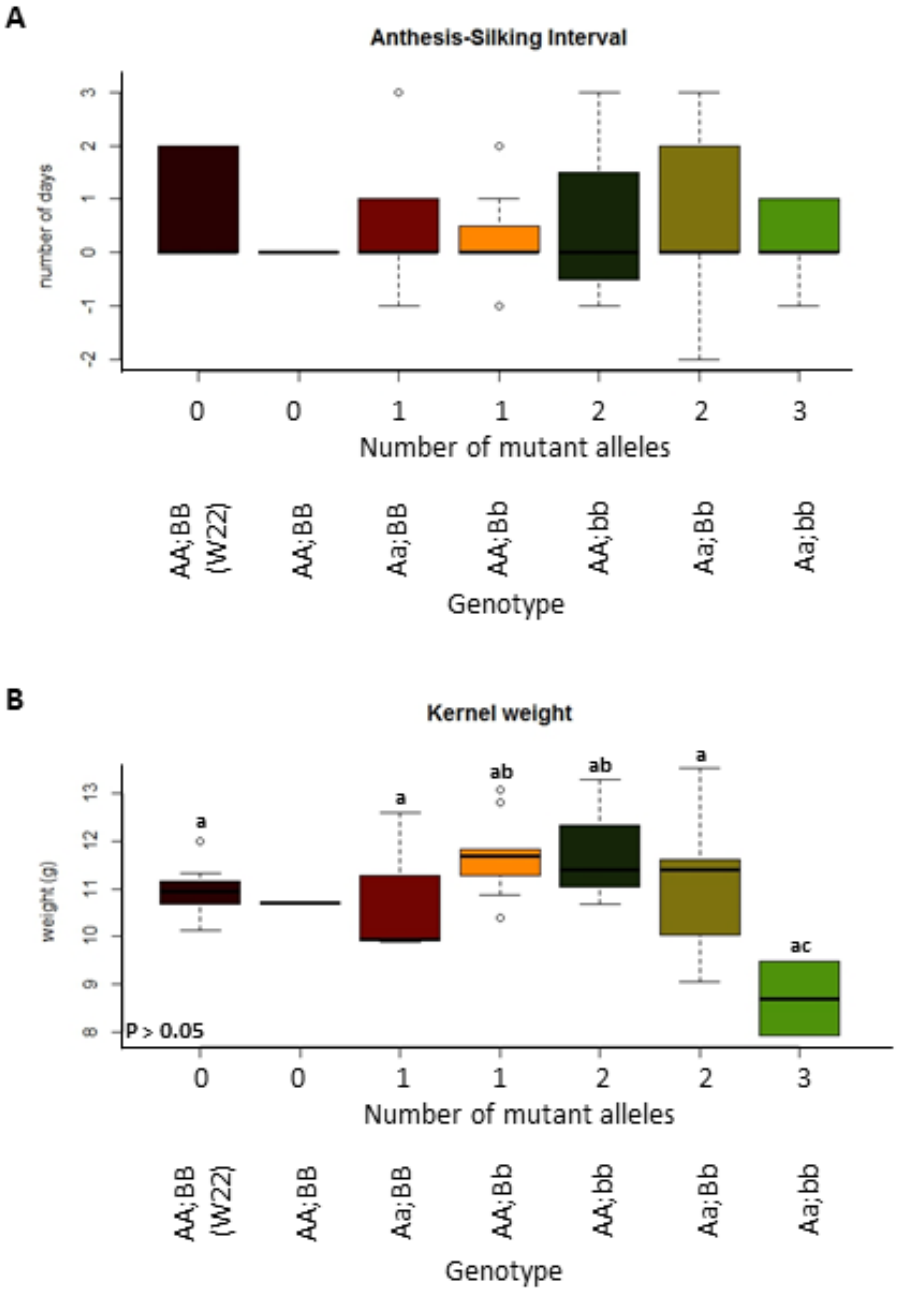

Figure 4.4: **Flowering time and kernel weight in *Zmmed12a/+;Zmmed12b/+* segregating plants.** Plants from segregating families grown in Puerto Vallarta field in 2016 were phenotyped. Six genotypic classes were found. AA;BB (W22) plants are the background in which mutants were induced, and were taken as a control. Genotypes are represented by letters A and B, for *Med12a* and *Med12b* genes, respectively. Capital letters denominate the wild type allele and the lower case letters denominate the mutant allele. Number of mutant alleles represents the total number of mutants alleles in each genotype. (A) Anthesis-Silking Interval is represented by the number of days to anthesis minus the number of days to silking. (B) Kernel weight represents the weight of 50 kernels for every ear. Different letters indicate significant differences between genotypes. A Tukey honest significant difference (HSD) test was used to determine significant differences ($P \leq 0.05$).

5 Discussion

5.1 Effect of the transposon insertions on *ZmMed12a* and *ZmMed12b* transcripts

Maize has two paralogous *Med12* genes, *ZmMed12a* and *ZmMed12b*. Mutant alleles for each gene were generated and designated as *Zmmed12a*-1::*Ds*, *Zmmed12a*-2::*Ds* and *Zmmed12b*-1::*Mu* (Martínez-Camacho, 2015; Núñez-Ríos, 2012). A semi-quantitative analysis was used to analyze the expression of *Med12* genes in the mutant alleles to evaluate the effect of the *Ds* or *Mu* insertions in gene transcription. To check how the *Ds* insertion affects the transcription of *Med12a* gene in *Zmmed12a*-1::*Ds* and *Zmmed12a*-2::*Ds* mutant alleles, two different sections of the transcript were analyzed. The first section shows the middle of the transcript, and the second one, a fragment near to the 3'UTR (Figure 4.1 A).

Here, it was found that *Med12a* gene transcripts in *Zmmed12a*-1::*Ds* mutant allele are clearly detected in both sections analyzed. *Med12a* transcription in this mutant allele looks like the observed in wild type plants; meanwhile, in *Zmmed12a*-2::*Ds* only the middle part of the transcript was evidently present, the 3'UTR showed a weak expression (Figure 4.1 B). In the case of first mutant allele, the *Ds* insertion apparently does not affect the expression of *Med12a* gene, but in the other mutant allele, *Zmmed12a*-2::*Ds*, *Med12a* transcript levels are strongly reduced after the *Ds* insertion (Figure 4.1 B). This shows that even when both alleles have *Ds* insertions (Figure 4.1 A), the effect on *Med12a* transcripts depends on the section where the insertion is located, since the *Ds* insertion in *Zmmed12a*-1::*Ds* mutant allele is in the 5'UTR, and in *Zmmed12a*-2::*Ds* it is in exon 10, a coding region (Figure 4.1 A), causing a reduction in transcript levels.

In many cases, as was shown in *Med12* mutants, transposon insertions generate mutants with different effects on gene regulation. Changes in gene regulation and their impact on phenotypes results from the position of TE insertion into a gene. This effect was previously seen after a large-scale *Ac* mutagenesis of the pink scutellum1 gene (Ps1), where multiple phenotypic classes were obtained, each with the TE inserted in different locations of the gene. Also, they showed that insertions close to the 3'UTR generated less strong phenotypes

than insertions in the middle of the gene (Bai et al., 2007).

In general, when TE are inserted in a coding region, changes in gene function are expected. Those changes may occur because of generation of stop codon or change in the open reading frame. In the case of *Zmmed12a*-2::*Ds* mutant allele the *Ds* insertion is in exon 10, and in *Zmmed12b*-1::*Mu* the *Mu* insertion is in exon 1. Only the *Ds* insertion was able to produce changes in gene transcription. But, of course, it is necessary to obtain or generate different alleles to better understand the functions of *Med12* genes. Since *Med12a* transcripts in the *Zmmed12a*-2::*Ds* mutant allele are evidently reduced by the *Ds* insertion (Figure 4.1 B), a phenotypic analysis was performed with this allele. The other mutant allele, *Zmmed12a*-1::*Ds*, was used to generate new insertions, as described below.

In the same way, the effect of the *Mu* insertion in the *Med12b* gene was analyzed. It was shown that *Med12b* transcripts in the *Zmmed12b*-1::*Mu* mutant allele are not affected (Figure 4.1 D). Primers SG174-SG175 flank the gene section where the *Mu* insertion is located (Figure 4.1 C), and it was found that both homozygous mutant for the insertion and wild type plants amplify the same size fragment (Figure 4.1 D). This behavior may be is observed because the *Mu* insertion is located near the 5'UTR, and the transcription machinery is not able to recognize the insertion, or because another factors are necessary to inhibit the gene expression. There is a kind of *Mu* mutants, called Mu-suppressible mutations, that allow the transcription within the Mu TIR, as it was observed in *Zmmed12b*-1::*Mu*. In these mutants, the inhibition of gene transcription is observed only when *MuDR* is present in the genome and can interact with the TIR (Barkan and Martienssen, 1991). But in that case a bigger transcript would be expected, and we found that the *Zmmed12b*-1::*Mu* transcript is wild type sized, suggesting that the insertion is being spliced out.

As shown before, the *Ds* insertion in the *Zmmed12a*-1::*Ds* mutant allele does not affect *Med12a* transcript levels. But, as the insertion is very close to the coding sequence of gene, it can be used to generate more and different alleles by re-mobilizing the *Ds* insertion into the gene. Since the *Ds* insertion is very close to the coding region, it is possible that the novel alleles obtained will have the *Ds* insertions in different parts of the gene. By this means, we can obtain alleles with the *Ds* insertion in the middle of the gene or at the end, so we can compare the effect of the insertion on *Med12a* transcripts, and also whether the new insertions confer mutant phenotypes.

5.2 *Zmmed12a* and *Zmmed12b* single mutants show some traits related to adaptation to phosphorous response

In order to characterize the root system, a phenotypic analysis was performed with the *Zmmed12a*-2::*Ds* mutant allele because of the clear effect of the *Ds* insertion on *Med12a* transcript levels, and with the *Zmmed12b*-1::*Mu* mutant allele. After here, I refer to the mutant alleles analyzed, *med12a*-2::*Ds* and *med12b*-1::*Mu* as *Zmmed12a* and *Zmmed12b* single mutants.

Zmmed12a and *Zmmed12b* single mutants were grown in full nutrient conditions. Phenotypic analysis was focused on root system architecture of the mutants for two reasons: 1.- In a previous work it was reported that some miRNAs that respond to phosphate starvation, like miR827, miR397, miR398, are up-regulated in Arabidopsis *med12* mutants grown in optimal phosphate conditions (Rodríguez-Medina, 2015). In addition, approximately 40 miRNAs involved in Root System Architecture (RSA) and morphogenesis, and 11 miRNAs that respond to environmental stress conditions showed expression changes, suggesting an important role of *Med12* in root development and in general, to environmental response (Rodríguez-Medina, 2015). 2.- The root phenotype of Arabidopsis *med12* mutants in normal phosphate conditions shows a shorter principal root, more root hairs, and longer lateral roots compared with a wild type plant, resembling more less a plant grown in phosphate-starvation conditions. When grow in phosphate starvation conditions, roots appear bigger, the principal root is longer, and mutants looks less affected by the stress compared with wild type plants (Martínez-Camacho, 2015). Again, these reports suggested that *Med12* is involved or is necessary for the correct response to environmental stresses.

In this work, in addition to the root architectural traits measured, some traits that are related to adaptation to phosphate-starvation were evaluated in maize *med12a* and *med12b* mutants, and showed interesting results. One of those traits was the root growth angle (RGA). RGA is an important trait that is involved in determining whether a plant develops shallow or deep roots, as it determines the direction of root elongation (An et al., 2017). Pictures were taken from different *Zmmed12a* and *Zmmed12b* mutant plants after 25 days of germination, and in those pictures RGA was determined by measuring the angle with respect to position of the soil. Plants with smaller angles are plants with shallower roots, and larger angles means plants with deeper roots.

It was found that both single mutants showed shallower root growth angle compared to W22 plants (Figure 4.2 C). Shallow roots are a desirable trait when plant breeding is focused on improving phosphate adaptation. Because of high Pi reactivity, and therefore its

low mobility in soils, topsoil layers have higher concentrations of Pi than subsoil layers. One plant strategy to response to phosphate starvation is the modification of the root system in order to enhance topsoil foraging (López-Arredondo et al., 2014). Shallower roots in *Zmmed12* mutants could increase their capacity to explore topsoil layers in which Pi is more abundant and therefore may improve Pi acquisition and development in low Pi conditions.

Another trait that showed an interesting behavior in maize *med12* mutants, in particular in the *med12b* mutant, was purple acid phosphatase activity (PAPs). These enzymes have a very important role in plant phosphorous nutrition, liberating phosphorous from organic sources in the soil and regulating the distribution inside the plant (González-Muñoz et al., 2015). They have been recognized as an important trait for adaptation to phosphate starvation, because in some Pi-efficient bean genotypes their expression is highly induced in comparison to non-efficient genotypes (Liang et al., 2010). Here, it was found that the *Zmmed12b* mutant shows higher levels of acid phosphatase activity compared with *Zmmed12a* and W22 plants grown in optimal phosphorous conditions (Figure 4.3 A). In maize, PAP expression is induced under low phosphate conditions (González-Muñoz et al., 2015). This suggests that *Zmmed12b* plants do not correctly perceive that the soil where they were grown contains all the nutrients available, conversely, maybe mutant roots perceive Pi-starvation and try to respond to it by producing high levels of PAPs to release Pi from the soil.

Coupled with the high acid phosphatase activity, it was found that phosphorous content is very different between *Zmmed12* mutants and W22 plants. In the case of *Zmmed12a*, high levels of P were found in the roots and normal levels in shoots compared with wild type plants (W22), but an opposite effect was observed in *Zmmed12b* mutants, in this case, it seems like *Zmmed12b* mutants over-accumulate P in shoots compared with the other two genotypes (Figure 4.3 B).

Pi homeostasis is regulated by different pathways, one of them is through microRNAs and sugars (Chiou and Lin, 2011). miR399 is the best characterized miRNA that is involved in the regulation of phosphate starvation: it is up-regulated in Pi starvation and directs the cleavage of the *PHO2* mRNA (Bari et al., 2006). *PHO2* is a ubiquitin-conjugating E2 ligase that acts on PHO1, a phosphate exporter involved in Pi transport from root to shoot by loading Pi into the xylem vessels (Liu et al., 2012). Arabidopsis and rice *pho2* mutants over-accumulate Pi in their leaves when grown in sufficient phosphate conditions (Delhaize and Randall, 1995; Wang et al., 2009a). Taking into account *Zmmed12* phenotypes, it is possible that *Med12* directly or indirectly regulate phosphate transporters or miRNAs involved in phosphate homeostasis. To further understand this regulation, we plan to investigate the expression pattern of a number of genes and microRNAs (e.g. ZmPho1,

ZmPht1, miR399, miR827) involved in maintenance of Pi homeostasis in *Zmmed12* mutants.

In addition, it will be informative to characterize the phenotype of *Zmmed12* mutants in low phosphate conditions. When different mutant lines are compared with W22 inbred line as a control, it is hard to make strong conclusions about the phenotype observed. Even if both mutants share the same background, each line has been maintained separately, and could accumulate diverse mutations. To deal with this, segregating families were generated.

5.3 Segregation distortion in *Zmmed12a/+;Zmmed12b/+* plants is observed across seed stocks in different field years

Families segregating *Zmmed12a/+*, *Zmmed12b/+* or both mutations *Zmmed12a/+; Zmmed12b/+* were planted in two field seasons, in 2016 and 2017, and in the greenhouse. Segregation ratios of different stocks were analyzed and compared. All showed segregation distortion no matter if segregating one gene or both genes together. Segregation distortion is defined as a deviation of the observed genotypic frequency from expected Mendelian segregation ratios (Sandler and Novitski, 1957).

In the 2016 field, progeny of two different *Zmmed12a/+;Zmmed12b/+* segregating families were grown, and the segregation ratios of the plants that germinated were analyzed. Sixty-six plants germinated and were genotyped. Six of nine genotypic classes expected were found (Table 4.2).

To increase the sample size, 140 seeds, that came from the same stocks planted in the field in 2016, were germinated in the greenhouse, and subsequently were genotyped and analyzed. I found that, when the number of plants increase, all the nine genotypic classes expected were recovered, but segregation distortion is still observed (Table 4.6). When each gene is analyzed separately, it is clear that the heterozygous class is over represented, the homozygous mutant class is half expected, and wild type class is very close to expected (Table 4.7).

To confirm if segregation distortion is present also different stocks, 90 seeds from 10 independent stocks segregating *Zmmed12a/+; Zmmed12b/+* were planted in the field in 2017. Two interesting points were found: 1.- Segregation distortion is observed in all 10 seed stocks used (Table 4.10). And 2.- If each gene is analyzed separately, segregation ratios are as observed in the plants grown in the field in 2016 and in the greenhouse (Table 4.7 and 4.11, respectively).

Stocks segregating only *Zmmed12a/+* or *Zmmed12b/+* were analyzed to determine if segregation distortion is a result of an interaction between both genes. One hunderd seeds from a single stock of *Zmmed12a/+* or *Zmmed12b/+* were grown in the greenhouse, and 90 seeds from 3 different stocks for each gene, were grown in the 2017 field. In both experiments, plants showed segregation distortion, although in greenhouse grown plants grown all genotypic classes were recovered (Table 4.4 and 4.5). Plants segregating *Zmmed12a* or *Zmmed12b* alone in the 2017 field showed similar segregation patterns between them: very few homozygous mutants or any, fewer heterozygous plants than expected and an increased number of wild type plants (Table 4.8 and 4.9). The number of heterozygous plants was higher than expected, the homozygous mutants was half than expected, and wild types was as expected in gene A, and fewer in gene B (Table 4.4 and 4.5).

Segregation distortion can result from differential inclusion in the products of meiosis, differential survival or fertilization success of haploid gametes, or differential survival of the diploid zygotes (Fishman et al., 2008; Fishman and Willis, 2005). The alteration of the normal process of meiosis with the consequence that a heterozygote for two genetic alternatives produces an effective gametic pool with an excess of one type is defined as meiotic drive (Sandler and Novitski, 1957). Meiotic drive can drastically alter the frequency of alleles in a population (Zimmering et al., 1970).

Segregation distortion observed in the single segregating stocks suggests that the segregation distortion is not because of a gene interaction, and also is not a result of the number of plants or an effect of seed stock because it was observed in both 2016 and 2017 fields, and in the greenhouse experiment.

To distinguish among male-specific, female-specific, and zygote-specific sources of transmission ratio distortion, a set of reciprocal backcrosses might be performed. The embryo-sac effect on segregation distortion can occur only when the heterozygous mutant is the female parent (Figure 5.1 A), if segregation distortion is observed in the progeny of this backcross but not in in male-segregating cross, this would be a female-specific segregation distortion source. Pollen competition occurs only when the heterozygous mutant is the male parent (Figure 5.1 B). Segregation distortion show in this backcross but not in the female-segregating backcross (Figure 5.1 A), would be a male-specific segregation distortion source. On the other hand, if segregation distortion is observed in the progeny of both, thus is zygotic-specific source.

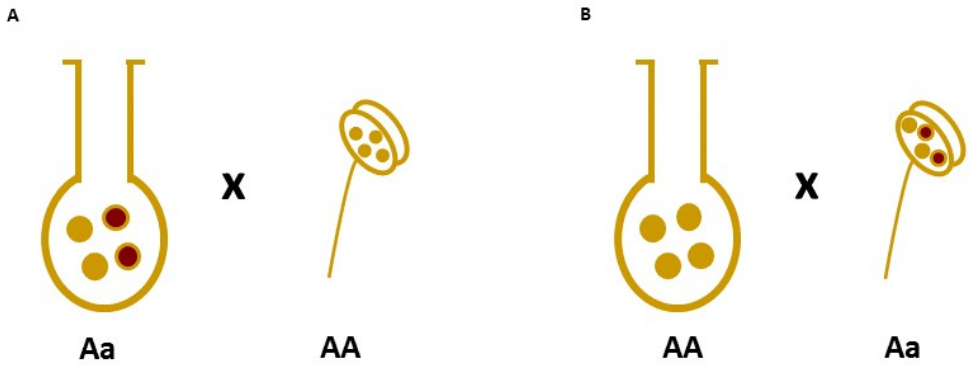

Figure 5.1: **Crosses strategy to distinguish different segregation distortion sources, male-specific, female-specific, and zygote-specific.** Backcrosses were develop from heterozygous mutant as female parent (A) or male parent (B). Wild type allele is indicated in yellow, and the mutant allele is indicated in red. Progeny of crosses will be genotyped, if segregation distortion is observed only in cross (A) is a female-specific defect. Segregation distortion only in (B) is a male-specific defect. But, if segregation distortion is observed in both crosses, there is a zygotic segregation distortion source.

.

Table 5.1: **Segregation ratios of plants segregating only *Zmmed12a* allele. Before perform crosses to generate the segregating families.**

Genotypes[a]	Expected	Observed	X^2 value	P-value*
AA	3.25	5	1.46	0.4
Aa	6.5	6		
aa	3.25	2		

[a]Genotypes are represented by letters A for *Med12a* gene.
∗Critical value of the X^2 distribution.
Capital letters denominate wild type allele.
Lower case letters denominate the mutant allele.

Finally, some points have to be considered to better understand the segregation distortion observed in *Zmmed12a/+;Zmmed12b/+* plants: 1.- The five plants that carry both transposon insertions came from a single cross between *Zmmed12a* (homozygous mutant for gene A) and *Zmmed12b/+* (heterozygous for gene B). It is necessary to analyze the progeny of other F1 families to discard the possibility that the segregation distortion observed is the result of a single event that happened in the F1 used here. Preliminary results showed that the segregation ratios of the stocks used to generate the *Zmmed12a;Zmmed12b* segregating

families present mendelian segregation ratios. Plants from a *Zmmed12a/+* single segregating family were germinated and genotyoped. Segregation ratios were as expected for normal mendelian segregation (Table 5.1), suggesting that the segregation distortion observed in the segregating families arises when the single mutants were crossed. 2.- Generate and analyze segregating families that came from the reciprocal cross, *Zmmed12b* as a female parent and *Zmmed12a* as a male parent. To determine the influence of the female background.

6 Conclusions

This thesis was focused on the genetic and phenotypic characterization of the two *Zmmed12a* and *Zmmed12b* single mutants, as well as *Zmmed12a/+;Zmmed12b/+* segregating plants.

The molecular characterization of the *Zmmed12a* and *Zmmed12b* mutant alleles showed that the effect of transposon insertions on *Med12* transcripts depends on the location of the *Ds* or *Mu* insertion. The phenotypic characterization of these single mutants showed that some traits related to adaptation to phosphorous response are active when grown in full nutrient conditions, suggesting that *Med12* is involved or is necessary for the correct response to environment. Regarding the *Zmmed12a/+;Zmmed12b/+* segregating plants, genetic analysis showed segregation distortion in all the stocks analyzed and different field years. Due to the segregation distortion it was hard to recover all the genotypic classes to perform a complete phenotypic analysis.

Bibliography

Ahmad, P. and Prasad, M. e. (2012). *Abiotic Stress Responses in Plants: Metabolism, Productivity and Sustainability*. Springer Science+Business Media.

An, H., Dong, H., Wu, T., Wang, Y., Xu, X., Zhang, X., and Han, Z. (2017). Root growth angle: An important trait that influences the deep rooting of apple rootstocks. *Scientia Horticulturae*, (216):256–263.

Backstrom, S., Elfving, N., Nilsson, R., and Wingsle, G.and Bjorklund, S. (2007). Purification of a plant Mediator from Arabidopsis thaliana identifies PFT1 as the Med25 subunit. *Mol. Cell*, 26:717–729.

Bai, L., Singh, M., Pitt, L., Sweeney, M., and Brutnell, T. P. (2007). Generating Novel Allelic Variation Through Activator Insertional Mutagenesis in Maize. *America*, pages 981–992.

Bari, R., Datt, P., Stitt, M., and Scheible, W. (2006). PHO2, microRNA399, and PHR1 define a phosphate-signaling pathway in plants. *Plant Physiol*, 141:988–999.

Barkan, A. and Martienssen, R. A. (1991). Inactivation of maize transposon-Mu suppresses a mutant phenotype by activating an outward-reading promoter near the end of Mu1. *Proc Natl Acad Sci*, (88):3502–3506.

Bennetzen, J. (1996). The Mutator transposable element system of maize. *Curr Top Microbiol Immunol*, 204:195–229.

Bennetzen, J. L. and Hake, S. C. e. (2009). *Handbook of Maize: Its Biology*. Springer Science + Business Media.

Bonser, A. M., Lynch, J. P., and Snapp, S. (1996). Effect of phosphorus deficiency on growth angle of basal roots in Phaseolus vulgaris. *New Phytol*, 132:281–288.

Buendía-Monreal, M. and Gillmor, C. S. (2016). Mediator: A key regulator of plant development. *Developmental Biology*, 419(1):7–18.

Calderón-Vázquez, C., Alatorre-Cobos, F., Simpson-Williamson, J., and Herrera-Estrella, L. (2009). *Maize under phosphate limitation. In J.L. Bennetzen, S.C. Hake, eds, Handbook of Maize: Its Biology*. Springer Science + Business Media.

Calderón-Vázquez, C., Sawers, R. J., and Herrera-Estrella, L. (2011). Phosphate Deprivation in Maize: Genetics and Genomics. *Plant Physiology*, 156:1067–1077.

Chen, Y.-F., Li, L.-Q., Xu, Q., Kong, Y.-H., Wang, H., and Wu, W.-H. (2009). The WRKY6 transcription factor modulates PHOSPHATE1 expression in response to low Pi stress in Arabidopsis. *Plant Cell*, 21:3554–3566.

Chiou, T.-J. and Lin, S.-I. (2011). Signaling Network in Sensing Phosphate Availability in Plants. *Annu. Rev. Plant Biol*, 62:185–206.

Delhaize, E. and Randall, P. (1995). Characterization of a phosphate-accumulator mutant of Arabidopsis thaliana. *Plant Physiol*, 107:207–213.

Devaiah, B., Madhuvanthi, R., Karthikeyan, A., and Raghothama, K. (2009). Phosphate starvation responses and gibberellic acid biosynthesis are regulated by the MYB62 transcription factor in Arabidopsis. *Mol. Plant*, 2:43–58.

Fishman, L., Aagaard, J., Tuthill, J., and Willis, J. (2008). Toward the evolutionary genomics of gametophytic divergence: patterns of transmission ratio distortion in monkeyflower (Mimulus) hybrids reveal a complex genetic basis for conspecific pollen precedence. *Evolution*, 62(12):2958–2970.

Fishman, L. and Willis, J. (2005). A Novel Meiotic Drive Locus Almost Completely Distorts Segregation in Mimulus (Monkeyflower) Hybrids. *Genetics*, 169(1):347–353.

Flanagan, P., Kelleher, R., and Sayre, M.H.and Tschochner, H. K. R. (1991). A Mediator required for activation of RNA polymerase II transcription in vitro. *Nature*, 350:436–438.

Gillmor, C., Silva-Ortega, C., Willmann, M., Buendía-Monreal, M., and Poething, R. (2014). The Arabidopsis Mediator CDK8 module genes CCT (MED12) and GCT (MED13) are global regulators of developmental phase transitions. *Development*, 141:4580–4589.

Gonzalez, E., Solano, R., Rubio, V., Leyva, A., and Paz-Ares, J. (2005). PHOSPHATE TRANSPORTER TRAFFIC FACILITATOR1 is a plant-specific SEC12-related protein that enables the endoplasmic reticulum exit of a high-affinity phosphate transporter in Arabidopsis. *Plant Cell*, 17:3500–3512.

González-Muñoz, E., Avendaño-Vazquez, Aida-Odette, C. M. R. A., de Folter, S., Andrés-Hernández, L., Abreu-Goodger, C., and Sawers, R. J. (2015). The maize (Zea mays ssp. mays var. B73) genome encodes 33 members of the purple acid phosphatase family. *Frontiers in Plant Science*, 6(341).

Griffiths, A. J., Wessler, S. R., Carrol, S. B., and Doebley, J. (2012). *Introduction to Genetic Analysis*. W. H. Freeman and Company.

Hamburger, D., Rezzonico, E., MacDonald-Comber Petetot, J., Somerville, C., and Poirier, Y. (2002). Identification and characterization of the Arabidopsis PHO1 gene involved in phosphate loading to the xylem. *Plant Cell*, 14:889–902.

Hochholdinger, F., Woll, K., Sauer, M., and Dembinsky, D. (2004). Genetic Dissection of Root Formation in Maize (Zea mays) Reveals Root-type Specific Developmental Programmes. *Annals of Botany*, 93:359–368.

Ito, M., Yuan, C., Malik, S., Gu, W., Fondell, J., Yamamura, S., Fu, Z., Zhang, X., and Qin, J.and Roeder, R. (1999). Identity between TRAP and SMCC complexes indicates novel pathways for the function of nuclear receptors and diverse mammalian activators. *Mol. Cell*, 3:361–370.

Jing-Wen, Y. and Gang, W. (2014). The Mediator complex: a master coordinator of transcription and cell lineage development. *Development*, 141:977–987.

Karthikeyan, A., Varadarajan, D., Mukatira, U., D'Urzo, M., Damsz, B., and Raghothama, K. (2002). Regulated expression of Arabidopsis phosphate transporters. *Plant Physiol.*, 130:221–233.

Kelleher, R., Flanagan, P., and Kornberg, R. (1990). A novel Mediator between activator proteins and the RNA polymerase II transcription apparatus. *Cell*, 61:1209–1215.

Khan, M. A., Gemenet, D. C., and Villordon, A. (2016). Root System Architecture and Abiotic Stress Tolerance: Current Knowledge in Root and Tuber Crops. *Front Plant Sci*, 7.

Kidd, B. N., Cahill, D. M., Manners, J. M., Schenka, P. M., and Kazanc, K. (2011). Diverse roles of the Mediator complex in plants. *Seminars in Cell and Developmental Biology*, 22:741– 748.

Kunze, R., Saedler, H., Lonnig, W., and Munchen, L.-m.-U. (1997). Plant Transposable Elements. *Advances*, 27.

Kunze, R. and Starlinger, P. (1989). The putative transposase of transposable element Ac from Zea mays L. interacts with subterminal sequences of Ac. *EMBO J*, 8:3177–3185.

Lazarow, K., Doll, M.-L., and Kunze, R. (2013). *Molecular Biology of Maize Ac/Ds Elements: An Overview. In Thomas Peterson, editor, Plant Transposable Elements, Methods and Protocols*. Springer Science + Business Media.

Li, Z., Xu, C., Li, K., Yan, S., Qu, X., and Zhang, J. (2012). Phosphate starvation of maize inhibits lateral root formation and alters gene expression in the lateral root primordium zone. *BMC Plant Biology*, 12(89).

Liang, C., Tian, J., Lam, H.-M., Lim, B., Yan, X., and Liao, H. (2010). Biochemical and molecular characterization of PvPAP3, a novel purple acid phosphatase isolated from common bean enhancing extracellular ATP utilization. *Plant Physiol*, 152.

Lisch, D. (2002). Mutator transposon. *TRENDS in Plant Science*, 7(11):498–504.

Lisch, D. (2013). *Regulation of the Mutator System of Transposons in Maize. In Thomas Peterson, editor, Plant Transposable Elements, Methods and Protocols*. Springer Science + Business Media.

Liu, T., Huang, T., Tseng, C., Lai, Y., Lin, S., Lin, W., Chen, J., and Chiou, T. (2012). PHO2-dependent degradation of PHO1 modulates phosphate homeostasis in Arabidopsis. *The Plant Cell*, 24(5):2168–2183.

López-Arredondo, D. L., Leyva-González, M. A., González-Morales, S. I., José, L.-B., and Herrera-Estrella, L. (2014). Phosphate Nutrition: Improving Low-Phosphate Tolerance in Crops. *Annu. Rev. Plant Biol.*, 65:95–123.

Lynch, J. P. (1995). Root Architecture and Plant Productivity. *Plant Physiol*, 109:7–13.

Lynch, J. P. (2007). Roots of the second green revolution. *Aust J Bot*, 55:493–512.

Lynch, J. P. (2011). Root Phenes for Enhanced Soil Exploration and Phosphorus Acquisition: Tools for Future Crops. *Plant Physiology*, 156:1041–1049.

Lynch, J. P. and Brown, K. (2001). Topsoil foraging: an architectural adaptation to low phosphorus availability. *Plant Soil*, 237:225–237.

Martínez-Camacho, C. (2015). Characterization of the MED12 subunit of Mediador in low phosphate responses in Arabidopsis thaliana. Master's thesis, Centro de Investigación y de Estudios Avanzados.

Martín, A., del Pozo J.C., Iglesias, J., Rubio, V., Solano, R., de La Peña, A., Leyva, A., and Paz-Ares, J. (2000). Influence of cytokinins on the expression of phosphate starvation responsive genes in Arabidopsis. *Plant J.*, 24:559–567.

McClintock, B. (1951). Chromosome organization and genic expression. *Cold Spring Harb Symp Quant Biol*, 16:13–47.

Misson, J., Thibaud, M. C., Bechtold, N., Raghothama, K., and Nussaume, L. (2004). Transcriptional regulation and functional properties of Arabidopsis Pht1;4, a high affinity transporter contributing greatly to phosphate uptake in phosphate deprived plants. *Plant Mol. Biol.*, 55:727–741.

Neumann, G., Massonneau, A., Langlade, N., Dinkelaker, B., Hengeler, C., Mheld, V., and Martinoia, E. (2000). Physiological Aspects of Cluster Root Function and Development in Phosphorus-deficient White Lupin (Lupinus albusL.). *Annals of Botany*, 85:909–919.

Núñez-Ríos, T. (2012). Molecular and genetic characterization of CCT/MED12 in (Zea mays). Master's thesis, Centro de Investigación y de Estudios Avanzados.

Núñez-Ríos, T., Ahern, K. R., Lepe-Soltero, D., García-Aguilar, M., Brutnell, T., Gillmor, C., and Sawers, R. (2017). Dissociation insertional mutagenesis of the maize Mediator CDK8 module gene ZmMed12a. *In prep.*

Pant, B. D., Musialak-Lange, M., Nuc, P., May, P., Buhtz, A., Kehr, J., Walther, D., and Scheible, W. (2009). Identification of Nutrient-Responsive Arabidopsis and Rapeseed MicroRNAs by Comprehensive Real-Time Polymerase Chain Reaction Profiling and Small RNA Sequencing. *Plant Physiol.*, 150:1541–1555.

Péret, B., Desnos, T., Jost, R., Kanno, S., Berkowitz, O., and Nussaume, L. (2014). Root Architecture Responses: In Search of Phosphate. *Plant Physiology*, 166:1713–1723.

Peterson, P. A. (2013). *Historical Overview of Transposable Element Research. In Thomas Peterson, editor, Plant Transposable Elements, Methods and Protocols.* Springer Science + Business Media.

Potters, G., Pasternak, T. P., Guisez, Y., and Jansen, M. A. K. (2009). Different stresses, similar morphogenic responses: integrating a plethora of pathways. *Plant Cell Environ*, 32:158 – 169.

Potters, G., Pasternak, T. P., Guisez, Y., Palme, K. J., and Jansen, M. A. K. (2007). Stress-induced morphogenic responses: growing out of trouble? *Trends Plant Sci*, 12:98 – 105.

Ribot, C., Wang, Y., and Poirier, Y. (2008). Expression analyses of three members of the AtPHO1 family reveal differential interactions between signaling pathways involved in phosphate deficiency and the responses to auxin, cytokinin, and abscisic acid. *Planta*, 227:1025–1036.

Rodríguez-Medina, J. (2015). Characterization of the MED12 subunit of Mediador in low phosphate responses in Arabidopsis thaliana. Master's thesis, Centro de Investigación y de Estudios Avanzados.

Samanta, S. and Thakur, J. K. (2015). Importance of Mediator complex in the regulation and integration of diverse signaling pathways in plants. 6(September):1–16.

Sandler, L. and Novitski, E. (1957). Meiotic Drive as an Evolutionary Force. *The American Naturalist*, 91(857):105–110.

Slotkin, R., Freeling, M., and Lisch, D. (2003). Mu killer causes the heritable inactivation of the Mutator family of transposable elements in Zea mays. *Genetics*, 165:781–797.

Sánchez-Calderón, L., López-Bucio, J., Chacón-López, A., Cruz-Ramírez, A., Nieto-Jacobo, F., Dubrovsky, J. G., and Herrera-Estrella, L. (2006). Phosphate starvation induces a determinate developmental program in the roots of Arabidopsis thaliana. *Plant Cell Physiol.*, 84:174–184.

Wang, C., Ying, S., Huang, H., Li, K., Wu, P., and Shou, H. (2009a). Involvement of OsSPX1 in phosphate homeostasis in rice. *Plant J.*, 57:895–904.

Wang, X., Wang, Y., Tian, J., Lim, B., Yan, X., and Liao, H. (2009b). Overexpressing AtPAP15 enhances phosphorus efficiency in soybean. *Plant Physiol*, 151.

Wei-Yi, L., Teng-Kuei, H., and Tzyy-Jen, C. (2013). NITROGEN LIMITATION ADAPTATION, a Target of MicroRNA827, Mediates Degradation of Plasma Membrane-Localized Phosphate Transporters to Maintain Phosphate Homeostasis in Arabidopsis. *The Plant Cell*, (25):4061–4074.

Zhang, Z., Liao, H., and Lucas, W. J. (2014). Molecular mechanisms underlying phosphate sensing, signaling, and adaptation in plants. *J Integr Plant Bio*, 56(3):192–220.

Zimmering, S., Sandler, L., and Nicoletti, B. (1970). MECHANISMS OF MEIOTIC DRIVE. *Annu. Rev. Genet.*, 4:409–436.

Appendix

1.- RNA extraction protocol

1. Grind frozen root tissue in liquid nitrogen.
2. Add 1200 μL of Trizol. Mix well. Incubate 10 min at room temperature.
3. Add 200 μL of chloroform and vortex very well, incubate 10 min at room temperature.
4. Centrifuge at 14 000 rpm in microcentrifuge, 4 °C for 15 min.
5. Remove aqueous (upper) phase and place in a new 1.5 mL tube.
6. Add 600 μL of 100 % isopropoanol. Mix and incubate at room temperature for 10 min.
7. Centrifuge at 14 000 rpm in microfuge, 4 °C for 15 min.
8. Discard supernatant. Add 1 mL 70 % ethanol. Centrifuge for 5 min, 4 °C, 8 000 rpm. Discard supernatant and air dry.
9. Re-suspend in 30 μL of DEPC water. Quantify by nanodrop. Run 1 uL on 1.5 % agarose non-denaturing gel to assay quality.

2.- Root acid phosphatase activity protocol

1. Grind 100 mg of tissue in a mortar.
2. Homogenize the tissue with 1 mL of MES buffer (MES 15 mM, $CaCl_2.2H_2O$ 0.5 mM, EDTA 1 mM) pH 4.5.
3. Transfer the homogenate into a new tube of 2 mL and centrifugate 20 min at 8000 g at 4 °C.
4. Transfer the clear supernatant into a new 1.5 mL tube and use it to measure the acid phosphatase activity.
5. Take 100 μL of clear supernatant and mix with 400 μL of MES buffer pH 4.5 containing BCIP (0.02% w/v).
6. Incubate the samples at 37 °C for 24 hr in darkness.
7. Add an equal volume of NaOH 0.25 M to stop the reaction. Mix by inversion.

8. Take 200 μL to measure the absorbance at 635 nm using a 96 well plate. Express the acid phosphatase activity as A635/gr tissue fresh weight/m.

3.- Total phosphorous content protocol

1. Clean completely th flasks with a solution of citric acid 2M, air dry them and take care that nothing touch the mouth of flasks.
2. Add 500 μL of HCl 1M to each flaks and fill them with distilled water without spilling and leave flasks overnight.
3. Discard the water of the flasks and wash them with distilled water 3 or 4 times, then put to constant weight into the oven at 65 °C overnight.
4. Take out the flasks and put into a desiccator, leave cool and and then weight them.
5. Put the tissue sample into the flasks and dry into the oven at 65 °C overnight.
6. Take out the flasks and weight them, then add 5 mL of the acids mix HNO_3/$HClO_4$ in a proportion 5:1 and leave digest the tissue overnight.
7. Warm the flasks to finish the to digest the tissue until dry the acids mix and get a white dust (ashes) in the bottom of the flasks.
8. Leave cool the flasks and then add 5 mL of distilled water to each flask and dissolve carefully the ashes. Incubate 2 min with the water
9. Add 2.5 mL of metavanadate and molybdate solution (Metavanadate 8.5 mM, Molybdate 125 mM, HCl 22.5 %). Incubate 10 min.
10. Add 5 mL of distilled water and incubate 20 min. Measure the absorbance at 400 nm.

    $*$ Total phosphorous content is calculated based on a standard curve.

4.- Rapid maize DNA extraction protocol for PCR

1. Grind frozen leaf tissue in 2 mL tube in Qiagen shaker.
2. Add 300 μL of extraction buffer (Tris pH 7.5 200 mM, NaCl 250 mM, EDTA 25 mM, SDS 0.5 %). Vortex to mix. Heat 68 °C 10 min.
3. Centrifuge at 13 000 rpm in microcentrifuge 7 min.
4. Transfer 200 μL of supernatant in 1.5 mL tube and add 200 μL of isopropanol. Mix gently.
5. Centrifuge at 14 000 rpm 5 min, discard supernatant.
6. Add 200 μL of 70 % ethanol.
7. Centrifuge at 12 000 rpm 5 min, remove ethanol and air dry for 3-5 min.
8. Re-suspend with 40-50 $\mu\mu$L of milliQ water.

5.- Primers used in this thesis

Primer	Sequence	Objective
A5.12 Fwd	AACGTGTAGACCTTGGGTTGAAT	Genotyping *Zmmed12a*-1::*Ds* allele.
A5.12 Rev	AGGCGTATAGCGGCTAAGGA	Genotyping *Zmmed12a*-1::*Ds* allele.
C2.7 Fwd	ACCCAGGAATCCACTCACTTTT	Genotyping *Zmmed12a*-2::*Ds* allele.
C2.7 Rev	TGCAATCAATAATAGCGTCCAG	Genotyping *Zmmed12a*-2::*Ds* allele.
SG174	AATAAAGGAGGTTGCGCTCAT	Genotyping *Zmmed12b*-1::*Mu* allele.
SG175	GAAGTACGGGATCTGGCTGA	Genotyping *Zmmed12b*-1::*Mu* allele.
JGp3	ACCCGACCGGATCGTATCGG	Detect *Ds* insertion.
JRS01	GTTCGAAATCGATCGGGATA	Detect *Ds* insertion.
Mu182	CGCCTCCATTTCGTCGAATCCCCTS	Detect *Mu* insertion.
TNC5	ACCTGTACAGAAGTCTGTTAAGCAA	Amplify the last fragment of exon 9 of *ZmMed12a*.
TNC4	CCATATGAGGAACTTCACTCCAG	Amplify the last fragment of exon 9 of *ZmMed12a*.
RS167	CCCCCACAGGCCCTAACTAAAACA	Amplify a fragment near the 3 'UTR of *ZmMed12a*.
RS170	CTGGCGAAAGCCTTTTTGAGAAGC	Amplify a fragment near the 3 'UTR of *ZmMed12a*.
SG176	TCCTCTCCCATCTTTTGTGG	Amplify a fragment of exon 9 of *ZmMed12b*.
SG177	TGCGAGATCATATGCACGTT	Amplify a fragment of exon 9 of *ZmMed12b*.
ZmCDk Fwd	GGAAGGTATGCACAGGACAGAT	Amplify a Cyclin-dependent kinasa gene used as constitutive gene.
ZmCDk Rev	TTCAGCACAATCTTGGCAAAAC	Amplify a Cyclin-dependent kinasa gene used as constitutive gene.